

Formation of aerosols in and after the flame

Dr. Anne S. Dederichs

*Department of Fire Safety Engineering
Lund University, Sweden*

Report 3136, Lund 2006

*Formation of aerosols
in and after the flame*

Dr. Anne S. Dederichs

Lund 2006

Abstract

Aerosols play an important role in fire spread and reduce visibility; the chemical and physical properties of aerosols are important for new approaches within fire detector development; furthermore their toxicity is a threat for human and environment. A lot of research is done on the formation of aerosols (soot particles and droplets). However, nowadays knowledge is fragmentary. This BRANDFORSK-report gives an overview on the existing research on formation of aerosols in fires and controlled combustion. It demonstrates that more coherent research is essential for fire safety engineering. The report lifts a series of relevant topics which need further study.

Keywords

Aerosols, Soot, Droplets, Fire, Combustion.

Report 3136

BRANDFORSK projekt 703-041

ISSN: 1402-3504

ISRN: LUTVDG/TVBB--3136--SE

Number of pages: 104

Illustrations: Anne S. Dederichs

Brandteknik
Lunds tekniska högskola
Lunds universitet
Box 118
221 00 Lund

brand@brand.lth.se
<http://www.brand.lth.se>

Telefon: 046 - 222 73 60
Telefax: 046 - 222 46 12

Department of Fire Safety Engineering
Lund University
P.O. Box 118
SE-221 00 Lund
Sweden

brand@brand.lth.se
<http://www.brand.lth.se/english>

Telephone: +46 46 222 73 60
Fax: +46 46 222 46 12

Contents

1	Introduction	1
1.1	Toxicity	1
1.2	Flamespread	3
1.3	Fire detection	3
1.4	Visibility	4
1.5	Non thermal damages	5
2	Fuels	7
2.1	Simple fuels	7
2.2	Complex fuels	17
3	Soot formation	23
3.1	Gas phase reactions	24
3.2	Inception of particles	24
3.3	Condensation	29
3.4	Surface growth	29
3.5	Coagulation	30
3.6	Agglomeration	31
3.7	Oxidation	32
4	Soot models	33
4.1	Empirical models	33
4.2	Semi-empirical models	35
4.3	Detailed chemical models	38
5	Aging	39
5.1	Surface growth	39

5.2	Methods of moments	50
5.3	Transition between coalescent to fractal regime	57
5.4	Sectional model of soot formation	62
5.5	Atmospheric aging processes	64
6	Heterogeneous reactions	67
6.1	Classes of heterogeneous reactions	67
6.2	Heterogeneous reactions in the flame	68
6.3	Heterogeneous reactions in the post flame	68
6.4	Heterogeneous reactions in atmosphere	69
6.5	Reduction of the formation of soot by heterogeneous reactions with additives.	69
7	Droplets	73
7.1	Six steps of droplet formation	75
8	Conclusion and opened questions	79
8.1	Fuels	80
8.2	Soot	81
8.3	Droplets	82
8.4	The complete fire model	82

Nomenclature

c	mol/m^3	Molar concentration
C_i	-	Cunningham slip factor
c_p	$J/kg K$	Heat capacity
d	m	Particle diameter
d^*	m	Critical particle diameter
D_i	m^2/s	Diffusion
D_{ij}	m^2/s	Diffusion
D_ℓ	m	Diameter of particles in section ℓ
D^f	-	Fractal dimension
E	J/mol	Activation energy
f	-	Branching coefficient
f_V	$m^3/(m^3)$	Soot volume fraction
g		Termination coefficient
g_0	$1/s$	Loss of nucleus due to collision of soot particles
h	-	Heaviside function
H	kJ/kg	Enthalpy
k_B		Stefan Boltzmann constant
$k_i, i = b, f$	(mol, s, m)	Reaction velocity of reaction i , backward or forward reaction
ℓ		Section

M	$1/m^3$	Statistical moment
\bar{m}_ℓ	m	Average mass of particles in section ℓ
$n_0(T)$	$1/s$	Rate of spontaneous formation of soot nuclei
N	$1/m^3$	Number density
N_ℓ	m	Number density of particles in section ℓ
PAH	–	Poly aromatic Hydrocarbon
$[P_{i,j}]$	mol/m^3	PAH-concentration of polymerization stage i and structure j
P	bar	Pressure
Q_ℓ	kg	Mass of section ℓ
r	m	Radius
R	$J/mol K$	Universal gas constant
S	m^2/m^3	Soot surface density
S_r	J/s	Radiation source
S_Ψ	$1/s$	Source term of variable Ψ
t	s	Time
TSI		Threshold sooting intensity
Y_i	kg/kg	Mass fraction for species i
X_i	mol/mol	Mole fraction for species i
$\mathbf{x} = (x_i, i = 1, 2, 3)$	m	Spatial vector
x_i	m	Spatial coordinate
Z	–	Mixture fraction
\tilde{Z}	–	Mean of the mixture fraction
$\widetilde{Z'^2}$	–	Variance of the mixture fraction

Numbers

Kn	-	Knudsen number
Le	-	Lewis number
Pr	-	Prandtl number

Greek

β		Collision frequency
ϵ	J/s	Energy dissipation
δ	m	Thershold diameter for fractility
Δ		Direction of trajectory in fractality space
λ	$W/m K$	Thermal conductivity
μ_τ	$kg/m s$	Dynamic viscosity
$\mu_{i,j}$	–	reduced mass
η	m^2/s	Characteristic kinematic viscosity
$\dot{\omega}$	mol/s	Reaction rate i terms of concentration
Ψ	–	Extensive variable
ρ	kg/m^3	Density
ρ_I	kg/m^3	Density
$\rho_s = 1860kg/m^3$	kg/m^3	Soot density

Preface

This project, (project no. 703-041) has been financed by BRANDFORSK. The project-manager was counseled by a reference group, with the following members:

Mats Bohgard, Prof. Aerosolteknik, LTH
Tommy Hertzberg, Svensk Provning
Lars Hellsten, Scania

This report starts out with presenting different problems related to fires and aerosols from and in fires. The goal with the project is to formulate a research-program which seeks solutions for these questions. The pilotstudy gives a literature overview in the fields:

- Formation and aging of soot particles
- Heterogeneous reactions in combustion processes
- Formation of droplets

The fields cover a large number of results from experiments and models. This report gives a overview over the domains and discusses single results which are considered relevant for going on in the field. The report starts out with an analysis of the research on fuel compositions and gas phase reactions, which are the basis of any combustion process leading to the formation of aerosols. The process of soot and droplet formation described and modeling approaches are presented. It must be said that even though soot is an important particulate emittant, it is not the only one. In the combustion of hay agglomerates containing the following species SiO_2 , Al_2O_3 , Fe_2O_3 , CaO , MgO , Na_2O , K_2O , SO_3 , TiO_2 , P_2O_5 were found [1].

The report tries to exploit the correlations of the processes of soot formation and droplet formation. This can be done since the formation of droplets can be considered as a heterogeneous reaction by adsorption onto soot particles.

At the same time the processes of soot and droplet formation can be modeled using the similar methods.

It was not possible to discuss every scientific result related to the field. Hence, the report neither covers combustion models (an overview can be found in [2]), such as flamelet models, nor the achievements made in modeling turbulent and laminar transport phenomena (for more information see [2, 3]). The chapter on droplets formation does not include sprays. Additional information on spray formation can be found in the BRANDFORSK report by Holmstedt et al. [4]. For further studies on spray combustion the author also recommends to read Gutheil et al. [5].

Chapter 1

Introduction

Aerosols occur in solid state and as fluids. The formation of particles and droplets in flames and heterogenous reactions with species from the gas phase play a role in a number of issues related to fire safety and the domain of fire technology. The relevant domains are described in this chapter. The following chapters summarize existing literature and visualize the need of further research for society is topic in the following sections. The focus of this chapter is the effect of aerosols on society.

1.1 Toxicity

90% of all mortalities in large fire are caused by detoxification. In smaller fires the fatality lays within 35%-50% [6, 7, 8]. Detoxification causes 1/3 of all nonfatal accidents [6]. The partition of detoxification incidents increases with decreasing number of deaths. One reason for this is the introduction of new materials in products. Some materials emit toxic species when being warmed up. Some older materials have recently been proven having toxic properties in fires [6]. A increased knowledge in pyrolysis processes and complex fuels are relevant in order to solve this kind of problems. Toxic properties of particles, such as soot, are subject of several studies [6, 2]. The particles themselves present a health hazard. They have the ability to penetrate the lungs and cause epidemiologic damages and may even provoke cancer. On the other hand soot particles are reactive and have the ability to adsorb and transport other toxic species.

Between 20 000 and 30 000 fires occur in Sweden every year in connection with accidents and exercises. Fires are responsible for 10 % of the total global

emission of particles, such as soot, to atmosphere [9]. As will be shown in this section, soot particles and their precursors, polyaromatic hydro carbons (PAH) present local pollutants.

Large amounts of saturated and unsaturated PAH are formed in fire. Their concentration are transient and dependent on the burning material, temperature and ventilation condition. As will be shown in later chapters, hydrocarbons occur as small molecules in fluid- and in gas phase. They are part of many materials which can be involved in fires. In the situation of fires they transform and form larger molecular structures and finally built PAH and soot particles. As will be shown in this section a long list of health effects are related to those emissions.

All carbon hydrates have anesthetic effects, which increases with the molecular size and concentration. Carbon hydrates are made responsible for cancer in lung, breast, intestine, bladder, skin and prostate [10, 11, 12].

Exposition to PAH can also cause problems with reproduction, kidney, immune system and developmental destructions (for further references see Ramesh et al.[13]), furthermore damages of the periferal neural system resulting in skeletal deformations, cramps, paralyzation of arms and legs ($n - C_6H_{14}$).

Small particles of about $4\mu m$ have the capability to enter the cellular. Nadziejko et al. [14] Exposition to large amounts of particles increases risk of thromboses and cardiological problems.

A large number of studies on diseases related to workers exposed to PAH have been summarized by Boffetta et al. [15]. Boffetta's survey over health and mortality studies in a number of countries lists work related diseases which coincide well with the health effects of PAH and soot, discussed in the previous paragraph. Humans working with gasification of carbon, with coke and combustion of diesel and workers in black carbon industries carry an increased risk for getting and dying of lung cancer.

But even other cancer types such as prostate, kidney and bladder occur more often amongst workers surrounded by large amounts of PAH. A large Swedish study on chimney sweepers by Gustavsson [16] map an increased risk in cancer in lung, liver, prostate, kidney, esophagus and skin. The studies mentioned above lets one assume that firemen and -women, who frequently are exposed to emissions of PAH and soot particles, carry a increased risk in the diseases mentioned. In order to prevent those work related damages it is important to gain more understanding in the building process of PAH and soot particles from different materials.

In their training and rescue work firemen and -women also belong to the group of workers who are exposed to PAH from incomplete combustion of many different materials.

The emission of PAH even affects flora and fauna. Phytotoxic effects of i.

eg. polyethylene has been detected [17] Most PAH do not bio accumulate but the dose for LC50(t) decreases with long term exposure. PAH's have differ in LC50 their transient development. Animal tests have shown that low doses of PAH can lead to damages in cells and lever [18]. According to recent studies soot particles affect the climate and greenhousegas [19].

Literature includes measurements of particles from fires [20]. The study shows that toxic isocyanates appear in particles from combustion of various fuels. This can lead to further detoxification of individuals, which can lead to a reduction in reaction time and may make evacuation impossible[21]. A larger knowledge on what particles are formed in fires, their numberdensity, size distribution and their reaction with other species is required.

1.2 Flamespread

Heat radiation from soot particles plays a major role in heat transition from the flame to the surroundings. Hence it contributes to flame spread. It has been shown that it is important to consider heat radiation from soot and larger molecules when determining flamespread [22, 23]. Contemporary studies focus on measuring particles in the post flame, a domain which does affect flame spread in a much smaller degree [9].

1.3 Fire detection

Reliable fire detection is important for evacuating and saving lifes as well as for preventing fires in further developing. False alarms imply high costs for society and insurance companies [24, 25]. A Swedish study from 2000 shows that 97% of all alarms where a mistake [26]. Three main problems within the field of fire alarms and fire detection can be identified:

- Different fire detectors do not respond in the same way on fires.
- The responds of a fire detector depends on the combustion condition.
- Fire detectors have the ability to react on emissions of particles and molecules originating from non combustion processes; i.e.g. dust, mist. They do not have the ability to *learn* and adjust to their surroundings.

In order to reduce the number of wrong alarms and avoid misdetections, more studies in the field of fire detection are a necessity. A few useful models for fire detection exist. One of them describe the response of a detector on the transport of the flow [27, 28]. The reaction time and the sensitivity of

the detectors models can only be improved if new models are developed that describe the time-development of several relevant parameters. Multi-variable detectors could be developed making use of such models. Research is required that describe the formation of such characteristic molecules and particles inside the flame. Schifiliti [29] states the need of smoke development in early stages of the flame in order to improve fire detection mechanisms. He describes the gap between today's demand on fire detection and existing models. Fire detector industry require more knowledge in the formation of aerosols, their transport and heterogeneous reaction of the particles with species from the gas phase. Furthermore an understanding is wanted that describes the time-development of particles and the change in their size, numberdensity and optical properties [30]. An analysis of several detectors can be found in literature [25, 29, 31]. Most detectors measure single parameters. The detectors react as soon as the critical parameters reach a well defined threshold. The parameters commonly applied in this context are numberdensity of particles or temperature. The fact that the parameters are affected by physics of the flow is not accounted for in today's detectors. Recent studies imply characteristics of the particles and the more complex properties of the fires should be applied in order to detect fires [32]. An other domain of relevance is the development of detectors with complex algorithms, that help the detector to adjust to different surroundings such as dusty or heated space [24, 31, 33]. Such a development would decrease the number of wrong calls. Detectors based on multisensors applying detailed information on chemical kinetics in the flame, temperature profiles and concentration of species, properties of the particles together with an development of intelligent algorithms can be expected to lead to an increase in precision of fire detectors.

More knowledge on what is going on inside the flame is required in order to achieve this goal.

1.4 Visibility

An increased numberdensity of the particles in fires result in an decreased visibility, which complicates and sometimes rules out the possibility for evacuation [34]. Different studies within BRANDFORSK and SFPE discuss questions of human behavior and evacuation in fires conditions [34, 35, 36]. Hence, an increased understanding of the formation of aerosols is even of interest for behavioral sciences [37] and for improving the chances for evacuation.

1.5 Non thermal damages

Smoke and particles cause material damages [38, 39]. Electronic equipment is most sensitive to dense clouds of particles, which appear in fires. BRAND-FORSK report [38] by Sören Isaksson describes several studies that show how particles, mostly soot, lead to corrosion, resulting in loss of metal and electrical overcharge and at times a collapse of the electrical circuit. Digital electronic have been proven to be more sensitive than analogous electronic. Isaksson concludes his report with a list of relevant future projects. Among these he expresses the need of developing models that describe the production and chemical properties of smoke and particles.

Chapter 2

Fuels

No matter if we seek to describe the combustion of gasses, fluids or solids, the combustion process happens through reactions in the gas phase. In the latter two cases the pyrolysis gas is formed before combustion takes place. All fuels are often categorized into two not very well defined groups: simple fuels and complex fuels. A definition of simple and complex fuel cannot be found in literature. In this report simple fuels are defined as a mixture of up to three combustible molecules in the gas phase with a low carbon number, carbon numbers of less than 10. The fuels burned in controlled combustion processes such as engines and incinerators as well as gases burned in uncontrolled combustion such as fires, are complex fuels. Complex fuels involve molecules with high carbon numbers (>10), mixture of different simple and complex fuels and other chemical substances. Different fuels differ in combustion efficiency and toxicity. The formation of particles simple fuels (section 2.1 and complex fuels will be discussed in this section. In order to be able to understand combustion processes in fires, relevant complex fuels need to be defined and their reaction mechanisms need to be developed. Section 2.2 will give an overview of composition of the pyrolysis gas of a selection of solid fuels, which are considered relevant in fires. Different models describing formation of particles from simple and complex fuels will be discussed in the following section.

2.1 Simple fuels

Most studies of chemical kinetics and fluid dynamics of combustion processes are performed applying simple fuels. Hydrogen (H), methane (CH_4) and ethylene (C_2H_4) have been popular fuels in this context. Nichols made one of

the first experiments on combustion be determining the temperature profile of acetylene (C_2H_2) [40], a molecule with high relevance for the formation of poly aromatic hydrocarbons (PAH) and soot.

2.1.1 Chemical Reactions

Different concepts are used in literature to model the formation of soot particles and their precursors, PAH, as well as other emissions from controlled and uncontrolled combustion. The generation of PAH can be described with chemical mechanisms which in some concepts are replaced with statistical methods. Chemical calculations are CPU time consuming. Limited CPU time is the reason that direct numerical simulations of combustion processes in relevant environments are possible. A compromise has to be made when processes of flow and chemistry are to be simulated. Hence, chemical mechanisms applied in literature can be divided into three groups:

- Simple reactions consider few step reactions involving a small number of chemical species. Those reactions are often applied in connection with CPU time consuming CFD calculations .
- Semi detailed reactions use about hundred species and thousand reactions. Often used coupled to calculations of
- Detailed reactions: imply ideally all possible reactions and engage several thousands of reactions. Even more reactions would be needed to model the growth of soot particles.

In order to limit the computational effort, some of those reactions are replaced by a statistical approach: the method of moments. This concept will be described in section 2.1.7.

Chemical Methods

The first steps to soot formation are chemical reactions of species present in the gas. Global reactions:



are broken down to elemental reactions of type



where A , B , C and D are species in the gas. The reaction rate by which A is produced in reaction (2.1) is a function of the concentrations of species A , $[A]$ and B , $[B]$ and the reaction coefficient k :

$$\frac{d[A]}{dt} = -k[A][B] \quad (2.2)$$

where the reaction coefficient k in low temperature domains can be defined through the Arrhenius form:

$$k(T) = A \exp -\frac{E_A}{RT}$$

for higher temperatures equation in the Non-Arrhenius form 2.3 is used

$$k(T) = AT^b \exp -\frac{E_A}{RT} \quad (2.3)$$

where T is the temperature, E the energy and R the universal gas constant. The species balance equation is solved for every species involved in the combustion process:

$$\rho \frac{\partial Y_i}{\partial t} = -\rho u_\alpha \frac{\partial Y_i}{\partial x_\alpha} + \frac{\partial}{\partial x_\alpha} \left(\rho D \frac{\partial Y_i}{\partial x_\alpha} \right) + \dot{\omega}_i$$

2.1.2 Simple chemical reaction mechanisms

One step reactions are used in detailed flow calculations when the chemistry is not a priority. CFD calculations can be CPU-consuming so that chemical reactions often are neglected. One such example is the work by Ravet et al. [41] where a complete chemical mechanism was substituted by one step reaction to be able to deal with combustion and aerodynamical phenomena simultaneously. Consequently, only two variables are needed to describe the problem. The one step assumption for simulating combustion chemistry is also taken by Huang, [42], where flow and flame calculations are coupled with acoustic models in order to determine the amplitude thermoacoustic limits cycle.

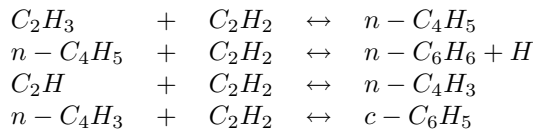
Soot models based on simple reaction schemes do not exist.

2.1.3 Semi detailed chemical reactions

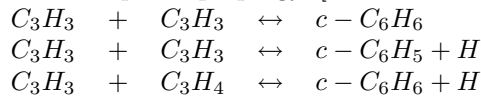
Reactions for chemical mechanism are built through relations described and listed by a large group of scientists and research institutes in Blauch et al. [43]. The work starts with simple O/H reactions and involve the formation and of larger molecules up to molecules with carbon numbers of 6.

2.1.4 Formation of PAH

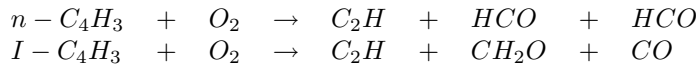
Large chemical mechanisms are involved when the first building stones for soot are the cyclic polyaromatic hydrocarbons benzene $c-C_6H_6$ and phenyl $c-C_5H_6$ are formed. The most mechanisms applied in this context base on a mechanism developed by Warnatz et al [44]. It includes H_2/O_2 -chemistry, $C_1 - C_4$ mechanism as well as the formation of $H_2 - CO$ and oxidation via O_2 and OH . The kinetic by Warnatz is valid for lean combustion conditions. In order to describe the formation of soot, the mechanism was adjusted (Frenklach et al. [45]) to rich combustion conditions which are of special interest for soot formation. Frenklach included a mechanism which leads to the formation of cyclic poly aromatic hydro carbons benzene and phenyl. The molecule mainly responsible for the process of growth of the rings is acetylene.



An other way for the formation of benzene in rich high temperature domains is via the species propargyl [46, 47, 48, 49]



Soot particles in flames are subjected to formation- as well as reduction processes. Oxidation via O_2 and OH is responsible for the reduction of the hydrocarbons formed during the formation of benzene and phenyl. Since flame velocities and species profiles are affected by these processes it is important to include a detailed description of the oxidation of higher order hydrocarbons. Slagle et al. [50], Warnatz [44] and Westmoreland [51] studied these processes. Another detailed chemical reaction scheme from Chiang et al. [52] and Balthasar was applied in the reaction mechanism [53].

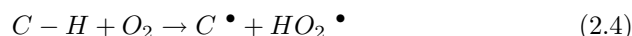


2.1.5 Growth of PAH

The process of soot formation is based on the chemistry of the small poly aromatic hydrocarbons (PAH) benzene $c - C_6H_6$ and phenyl $c - C_6H_5$. The growth of PAH's is a chemical process, beginning with one stable PAH. The process could be described with a large chemical mechanism.

2.1.6 Detailed chemical reactions

Nowadays large detailed combustion mechanism can automatically be generated. Software is developed to automatically produce reaction schemes containing ten thousands of reactions and thousands of chemical species [54, ?, 55]. The reactions are formed through analogies with known reactions as cited in section 2.1.3. A mechanism scheme is generated by sorting types of reactions in reaction classes. Reactions are defined through the reaction patterns, molecular substructures such as hydrogen abstraction from carbon. A corresponding pattern is



applied on benzene the reaction becomes:



In general the reaction can be applied on all carbon radicals included in any molecular structure.

The automatic generation of mechanism has made it possible to describe combustion of fuels up to heptane [55]. The reaction rate is defined through position of the hydrogen atom and the symmetry.

2.1.7 Reduction of mechanisms

In any modeling of combustion processes reactions are represented through conservation equations. Every reaction consumes CPU time and the relevance of each reaction path varies with condition of the combustion process. In order to reduce the computational afford and memory the application of detailed mechanism is often coupled to reduction techniques. The challenge of such technique is not the simplification of the chemistry involved, but rather the reduction in the complexity of the mathematical form [45]. The relevance of reaction pathes alter with the combustion condition, so that they may be ignored at certain stages while they must be included in others. Different methods reduction apply different selection filters on the respective mechanism. Besides reduction prior and during calculation some methods apply reduction techniques for compression of data resulting from chemical calculations. A number of reduction techniques result in increased CPU consumption due to convergence problems, caused by a change in Jacobian. Post-process data compression methods do not suffer from these problems. Some reduction techniques are described in the following subsections.

Sensitivity analysis

A sensitivity analysis [44] can be coupled prior to the reduction of a detailed mechanism. The goal of such an analysis is to investigate the correlation between the concentration of species i to the rate k_r of reaction path r, i . The sensitivity of path r in respect to the concentration of species i is given by:

$$E_{i,r} = \frac{\partial c_i}{\partial k_r} \quad (2.6)$$

A sensitivity analysis can identify rate limiting reactions and thereby give a deeper understanding of the reaction system.

ISAT

Computationally efficient implementation of combustion chemistry using *in situ* adaptive tabulation (ISAT) has been undertaken by Pope [56]. The method is based on tabulating the physical and chemical evolution of combustion processes in a condensed way.

Neural networks

Neural networks coupled to Pope's ISAT method [56] has been applied by Chen et al. [57] to reduce storage space of chemical kinetic data by more than a factor of 100.

ILDm

Intrinsic low-dimensional manifolds (ILDm) described by Maas and Pope [58, 59, 60, 61] define the time evolution of one species as a function of other major species thereby reducing computation time and memory requirements. Limiting factors which should be considered in this context are the CPU time required to generate the memory of the generated data, the error associated with the reduction process, the CPU time required to retrieve the filtered data, and the applicability of the method.

MARS-method

The multi-adaptive regression spline or so-called MARS method, developed by Friedman [62] offers flexible regression modelling of high-dimensional data. It makes use of spline basis functions and tunable parameters such as order and knot locations using a recursive partitioning approach. It is capable of modelling multivariable interactions.

Adaptive chemistry

Adaptive chemistry is the application of reduced chemistry models for different conditions within the flame. It can be used as a postprocessor. In order to achieve reasonable results within a reasonable amount of CPU time one needs to define validity criteria for each model to appropriately switch between mechanisms. Literature lists a number of adaptive chemical models. Schwer et al. [63] modeled an H_2/O_2 shear layer diffusion flame and two axisymmetric, co-flowing methane/air laminar flames. The adaptive chemical model was compared with calculations performed with a full scale chemical mechanism. Each reduced model was used only under the most suitable reaction conditions. A number of reduced mechanisms are then constructed which are valid for specific reaction conditions. The reduced mechanisms are subsets of the complete mechanism. In the reduction process reactions and species, which are considered unimportant in certain regions of the flame, are excluded from the calculation. Each model is valid for a specified range of temperatures, pressures, and species mass fractions. The reduction process applied by Schwer et al. is a composition of a concentration-criteria, additional validity criteria distinguish high-temperature and low-temperature models, fuel-rich and fuel-lean models and regions where chemical reactions can be neglected entirely. The full mechanism was only applied in a very small region.

Adaptive chemistry has even been applied in the flamelet model [2]. A detailed chemical mechanism containing 66 species was used to calculate species concentrations in a turbulent ethylene/air flame using the unsteady flamelet model. In this calculation species with a short lifetime $2 \cdot 10^{-6}$ s were excluded from the calculation. Thirty-nine species could be removed from the calculations. An online reduction principle was applied in these calculations.

Lumping

The method of lumping covers two approaches: linear and non-linear lumping. Both methods present simplifications useful in detailed modeling approaches.

Linear lumping Frenklach [45, 64] divided the growth of PAH into different stages, associated to different size classes of PAH. The steps of growth from one size class to the next are assumed to be identical. The reversible reactions repeat in cycles of growth (figure 2.2). The mechanism can be restricted to the so called *HACA*-mechanism 2.1.7, which is a reversible reaction scheme. It describes the growth of a PAH by hydrogen abstraction through reaction with H , O or OH , acetylene addition, a second hydrogen abstraction followed by an acetylene addition, which completes the next ring on the PAH (figure 2.3).

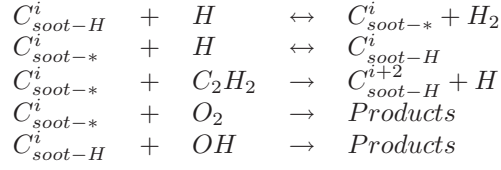


Figure 2.1: HACA scheme

The statistical method of moments solves the size distribution. One general reaction rate $P_{i,j}$ is related for the translation from one stage to the next. i denotes the size class and j one chemical structure in the polymerization cycle. The resulting set of equations has the dimension of the number of distinct chemical structures within one cycle. Mauss [65] suggested to reduce the system even more by introducing the method of fast polymerization which implies that the PAH's are in steady state.

$$\frac{\partial [P_{i,j}]}{\partial t} = 0 \quad (2.7)$$

This approach reduces the polymerization reactions and thereby the computational effort for the calculation of the moments of the size distribution. The r^{th} moment of the PAH size distribution is defined as:

$$[M_r^{PAH}] = \sum_{i=1}^{\infty} \sum_{j=1}^6 n_{i,j}^r [P_{i,j}] \quad r = 0, 1, \dots, \infty \quad (2.8)$$

where $n_{i,j}^r$ is the number of monomer units, which is one C-atom and $[P_{i,j}]$ the concentration of the PAH structure j at stage i . The transport equation for the density weighted moments \overline{M}_r^{PAH} for a laminar premixed flames was given by [53].

$$\rho v \frac{\partial \overline{M}_r^{PAH}}{\partial x} - \frac{\partial}{\partial x} (\rho D_1) \frac{\partial}{\partial x} \overline{M}_{r-2/3}^{PAH} = \sum_{i=1}^{\infty} \sum_{j=1}^6 n_{i,j}^r L(\overline{Y}(P_{i,j})) \quad (2.9)$$

where $L(\overline{Y}(P_{i,j}))$ is the convective diffusive operator of the PAH moment continuity equation:

$$L(\overline{Y}(P_{i,j})) = r_{pi} + r_{con} + r_{reac} \quad (2.10)$$

It is balanced by the source terms of particle inception, condensation and the chemical reactions. This method neglects the interaction of polymer species.

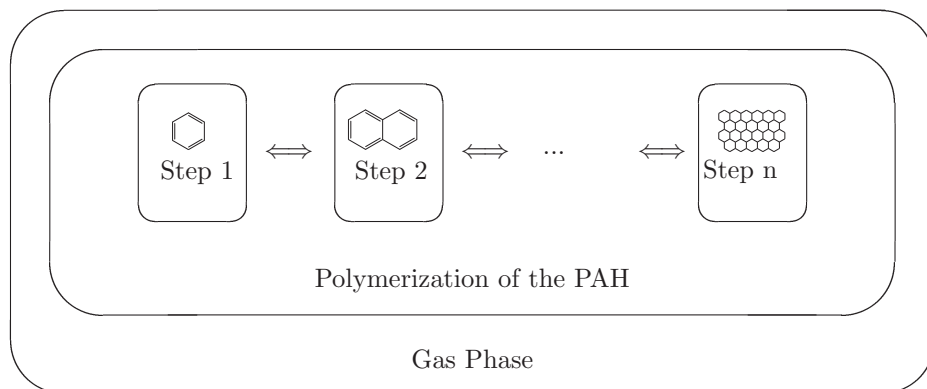


Figure 2.2: The growth of PAH by the method of linear lumping

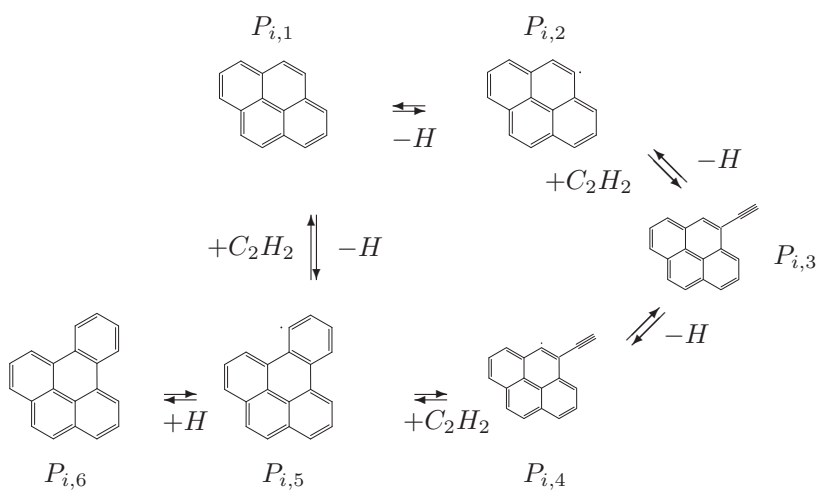


Figure 2.3: HACA mechanism of growth

Non-linear lumping: Many species are involved in the description of the gas phase chemistry. Even more reactions would be needed to model the growth of soot. In order to save CPU time, some of those reactions are replaced by the statistical method of moments: The process of growth is divided into discrete classes. The method of moments [66] is applied to describe the distribution of the size classes, the stages of growth.

Moment r of the size class M is defined to be a sum of the probability density function and size distribution:

$$M_r = \sum_{i=1}^{\infty} x_i^r p_i \quad (2.11)$$

where x_i^r is the random variable, the particle, the PAH and p_i probability density function. The physical interpretation of the variables will be discussed in the following sections. The method of moments is valid, if the sum converges. The first and second moments are of special meaning. The first moment

$$M_1 = \sum_{k=1}^{\infty} x_k p_k$$

is the expectation value of M and the second moment

$$M_2 = \sum_{k=1}^{\infty} x_k^2 p_k$$

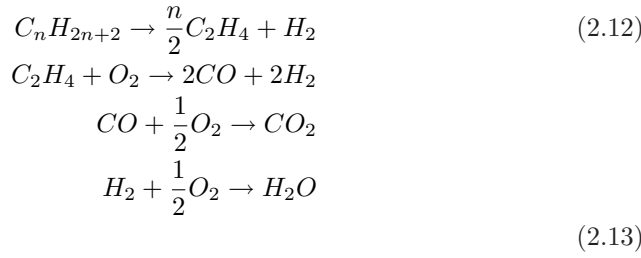
is the variance of M . They even may be interpreted in a physical context as will be shown in chapter 3. This method takes into account interaction of polymer species.

Fitting

Fitting of processes is applied for reduction of the reaction scheme into a few steps. It should be mentioned that fitting also is used to minimize the storage of chemical data resulting from models [2]. The following two paragraphs are taken from [45].

Empirical fitting Empirical fitting implies the development of few step mechanism and a description of the reaction rate, which is general for the system. Hautman [67] formulated such a mechanism for propane combustion.

The mechanism reads:



The empirical reactions are fitted into the following general expression for the reaction rate:

$$\dot{\omega} = A e^{-\Theta/T} \prod_i C_i^{\beta_i} \quad (2.14)$$

A , Θ and β_i are fitted parameters. This approach reduces the overall validity of the resulting combustion model to one condition.

Reduction by Approximation This method implies deciding larger mechanisms into a number of subsets. Reaction steps are formulated, representing the stoichiometry of each subset [68, 69].

Postprocessing

The discrete wavelet transform (DWT) presents as filter applicable to data fields, using a recursive partitioning approach. Another application is in the reduction of the differential equations [70].

2.1.8 Hardware programming

Developments in the field of electronics lead to an decrease in CPU time. One way to shorten the computation time even more could be the translation of the complex CFD programs into hardware description languages such as VHDL, which directly are synthesizable on an FPGA chips [71].

2.2 Complex fuels

Complex fuels take part in real combustion situations as in fires. The identification of fuels involved in fires is essential for model development. The work can be considered as an extension of modeling the combustion of simple fuels.

Complex fuels are not clearly defined in literature. Hence, in this report complex fuels are defined as being fuels that fulfill one or more of the statements below:

- carbon number of higher than 10.
- molecules containing other atoms than carbon hydrates.
- containing more than one species.

Until now this process has been subject of experimental studies alone. Some studies will be presented in the following subsection 2.2.1.

2.2.1 Defining complex fuels

Literature contains a few definitions of fuels for biomass combustion [72, 73, 74]. Some results are discussed in the following subsections.

Birch wood

In her research Svenson [72] identified main components in the pyrolysis of single particles.

Experimental setup The measurement was done by using a SPAR apparatus, which consists of a furnace heatable up to 1000°C and an adjustable fall tube. The reactor was heated with five u-shaped heating elements symmetrically situated around a sample holder. The pyrolysis starts as soon as the particle (in our case 200 mg birch wood) lands on the holder. The gas analysis was performed using a molecular beam mass spectrometer (MBMS) apparatus [72].

Results Svenson determined the decomposition kinetics, surface temperature and studied samples of emitted gases both inside and outside the particle surface. The combusted material takes part in fires and biomass combustion. The qualitative result of her work lead to the detection of the following 20 species: H_2O , CO , CO_2 , C_2H_2 , C_2H_4 , C_2H_6 , C_3H_6 , C_3H_8 , CH_3OH , $\text{C}_2\text{H}_5\text{OH}$, HCHO , CH_3CHO , HCOOH , CH_3OOH , HCOOCH_3 , $\text{C}_3\text{H}_6\text{O}$, levoglucosan (a sugar anhydride), glycolaldehyde and furan. Figure 2.4 shows gas emission signals as a function of temperature for the pyrolysis of a birch wood particle subjected to an rising temperature. The temperature increase was $50^{\circ}\text{C}/\text{min}$. The temperature range for the pyrolysis process was $350 - 500^{\circ}\text{C}$. The profiles show a qualitative result of the composition of the emitted gas.

Agricultural residues, Birch, wheat straw

At KTH in Stockholm a group of scientists of Emilia Björnbom [73, 74] performs analysis of different combustible materials in a screw feeder that allows particles to move through the reactor with $250g/h$. The composition of the cleaned gas was measured using a GC-chromatograph. CO_2 , H_2 , CO , N_2 , CH_4 , and hydrocarbons up to C_7 were detected. Table 2.2.1 shows the concentration of selected components of the gas from olive waste particles, wheat, untreated and pelletized straw as well as birch wood particles. The distribution considers different particles sizes and temperatures.

Table 2.1: Gas composition of different biomass materials (bdl: below detection limit), with courtesy from Bjornbom et al. [73].

Composition of the gaseous products (vol% Nitrogen and waterfree basis)											
Biomass	Straw		Straw pellets		Olive waste		Wood: birch				
\varnothing (mm)	0.5 -1.0		0.5-1.0		0.5-0.8		0.8-1.0		0.5-0.8		0.8-1.0
T (100°C)	8	10	8	10	8	10	8	10	8	8	10
H_2	35.0	43.9	24.2	38.8	15.8	32.1	12.8	21.1	17.3	16.8	34.0
CH_4	9.5	4.8	16.2	8.0	24.1	13.5	24.1	18.3	15.7	16.2	11.7
$C_2H_2; C_2H_4$	3.1	bdla	4.7	0.1	3.4	0.3	3.9	0.5	5.8	6.2	0.5
C_2H_6	0.1	bdl	0.5	bdl	0.7	0.1	0.9	0.2	0.3	0.3	bdl
C_6H_6	0.6	0.1	0.7	bdl	0.6	0.2	0.5	0.2	1.2	1.2	0.6
CO_2	23.7	5.0	19.3	4.7	15.7	8.6	18.2	12.3	9.6	8.3	7.5
CO	28.0	46.2	34.4	48.4	39.2	45.2	40.1	47.4	50	50.7	45.7

Other biomass materials

The distribution of H_2 , CH_4 , CO and CO_2 from grape and olive bagasse in a temperature interval of $[300, 900]^\circ C$ was determined by [75]. Research results determining the emission of dioxin from treated and untreated woodchips and pellets from beech, beach, pine, bark, conifers, aspen, maple, spruce, differently treated plywood, and even coal and hay, straw ad waste wood has been summarized by Elena Lavric [76].

Polymeric materials

A rough description of relevant polymers is given in the latest SFPE handbook [77]. Polymers are classified into X groups [77]:

- Carbonaceous polymers with no heteroatoms:
 - polyolefins, which are thermoplastics
 - * polyethylene
 - * polypropylene
 - polydienes are elastomeres
 - * polyisoprene synthetic or natural rubber
 - * polybutadiene, a rubber substitute
 - * other copolymers appearing in ABS (acrylonitrile butadiene styrene styrene terpolymers), SBR (styrene butadiene rubbers), MBS (methyl methacryl butadiene styrene terpolymers), EPDM (ethyl propylene diene rubbers)
 - aromatic hydrocarbon polymers, based on polystyrene
- oxygen-containing polymers
 - cellulosics have a big relevance in fire
 - * wood and paper products
 - * Used in PMMA (poly methyl methacrylate)
 - polyacrylics only oxygen-containing polymers containing carbon atoms
 - polyesters are manufactured from glycols
 - * polyethylene terephthalate (PET)
 - * polybutylene terephthalate (PBT)
 - * ...
 - other oxygenated polymers include phenolic resins, polyethers and polyacetals (polyformaldehyde used for its hardness)
- Nitrogen containing materials
 - nylons
 - polyuretans (PU) applied in building materials as foam for thermal insulation.
 - polyamid
 - * natural: Wool, silk, leather
 - * synthetic aromatic polyamides: textiles for clothing
 - polyacrylonitrile
- Chlorine containing polymers

- polychloroprene used for wire and cable materials and resilient foams
- poly vinylidene chloride (PVDC) for films and fibers
- Flourine containing materials

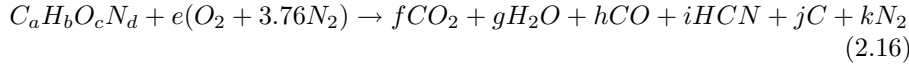
The thermal composition containing the emission of a few species from some of the materials can be found in the work by Beyler.

2.2.2 Simple chemical reactions

In spite or because of the complexity of the problem many fire codes reduce the total of all chemical reactions to one step reactions such as:



The local concentration of a few toxic chemical species are introduced by the direct relation to one parameter only, which in some codes is the ventilation condition and in others the mass of burned solid fuel. An example can be found in Wade et al. [78]



where:

$$a = f + h + i + j \quad (2.17)$$

$$b = 2g + i \quad (2.18)$$

$$c + 2e = 2f + g + h \quad (2.19)$$

$$d + 7.52e = i + 2k \quad (2.20)$$

Soot formation:

$$\frac{\Psi_{s,v}}{\Psi_{s,wv}} = 1 + \frac{\alpha}{\exp(2.5 \cdot \phi^{-\xi})} \quad (2.21)$$

The following correlation for the dependence of the soot yield on the global equivalence ratio was developed by Tewarson, Jiang and Morikawa [22, 23] where s, v is the soot yield under ventilated controlled conditions, s, wv is the soot yield under well ventilated conditions, ϕ is the global equivalence ratio, and α and ξ are constants dependent on the fuel.

$$\Psi_{CO} = \frac{a}{\pi} \tan^{-1}[10(\phi_\epsilon - b)] + c \quad (2.22)$$

where a,b and c depend on the layer temperature.

The concentration of oxygen is mostly assumed to correspond to the amount of oxygen needed to burn the fuel [79].

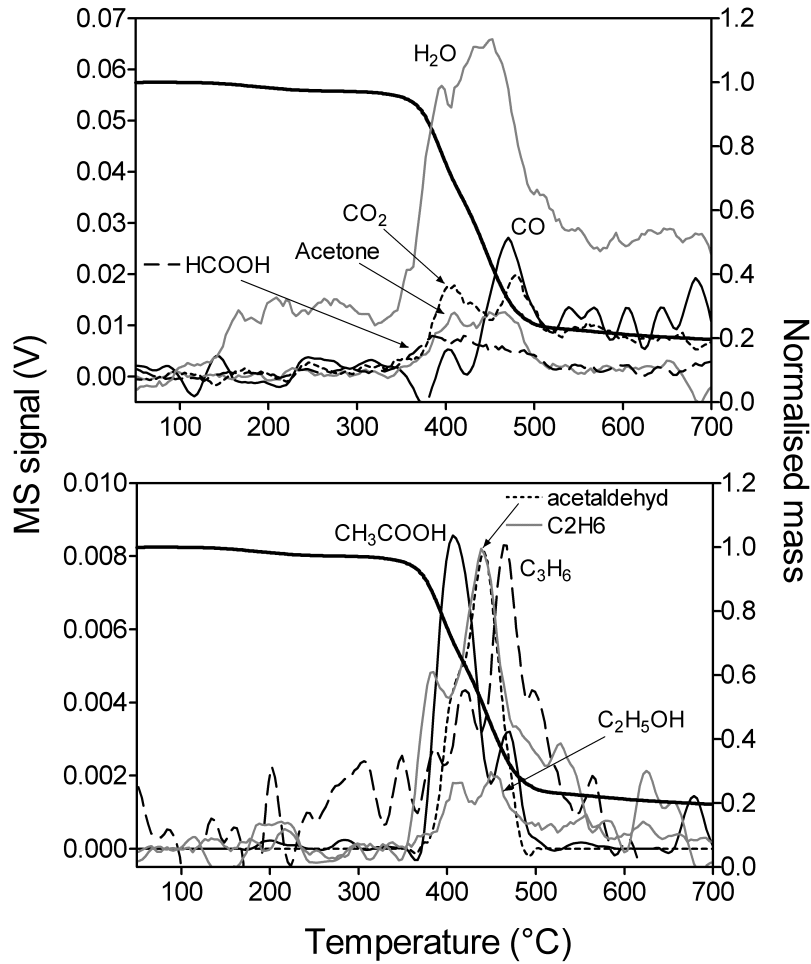


Figure 2.4: Mass loss and gas emission data as a function of temperature for pyrolysis of birch wood subjected to $50^{\circ}\text{C}/\text{min}$ temperature increase, with the courtesy of Jenny Svenson [72].

Chapter 3

Soot formation

Soot is an agglomerate of particles, which vary in structure and size [80]. The main constituent of soot is carbon and some minor amounts of hydrogen and oxygen. Depending on the surrounding gas, soot particles adsorb other species on the surface. Even though many properties of soot have been identified, it has not been possible to uniquely defined the chemical composition of soot.

McKinnon et al. [81] defined the smallest soot particle according to the limits of an electron microscope can detect. It has a size of $2000 \text{ \AA} = 20 \text{ nm}$. Figure 3.1 shows the electron microscopic picture of soot particles from wood chips pyrolysis produced at the Denmark's Technical University [82]. Soot is produced during the combustion of hydrocarbons under fuel rich conditions at high temperatures. The emission of soot from a flame is determined by the formation and oxidation of soot. This process is divided into seven steps: particle inception, condensation, surface growth, fragmentation (the reverse of surface growth), coagulation, agglomeration and oxidation. Soot models of today describe the formation of soot in seven steps (figure 3.2). The different steps in soot formation dominate the different zones in the flame. Figure 3.3 is taken from Megaridis and Dobbins [83]. It shows that the zone down stream in the flame is dominated by inception and condensation of PAH's previously formed in the gas phase. Those are the first soot particles. The surface of the particles grow in the reaction with C_2H_2 . They coagulate and build large agglomerates. At high temperature the soot particle interacts again with the gas phase and oxidation contracts the size of the particle. This figure is very schematic and does not tell the complete truth. At first the sources have a smooth distribution and affect the process of soot formation simultaneously. The single zones of soot formation are dependent of the mixture fraction scalar dissipation rate and enthalpy [2]. Soot formation occurs even on the horizontal

plane of the flame.

other studies show the existence of other paths for the formation of agglomerates than the paths described in the following sections. The results can be found in research on fires and the combustion of biomass [1]. They discuss the so called in-bed-agglomeration, a process of melting of the heated material followed by freezing into agglomerates. The species never enter the gas phase. The particles formed in the experiments involve other chemical species than carbon and hydrogen.

3.1 Gas phase reactions

Reactions in the gas phase The first step to soot formation is the formation of cyclic benzene $c - C_6H_6$ and phenyl $c - C_6H_5$ in the gas phase. The cyclic molecules grow further into two-dimensional Poly Aromatic Hydrocarbons (PAH).

3.2 Inception of particles

Particle inception describes the initial step of soot formation in which the first particle is formed. The gas phase is left behind and the phase of condensed material is entered when two two-dimensional PAHs merge and form the first three-dimensional structure. The size of this first particle is still a matter of discussion. As mentioned above the latest experimental techniques are used to define the smallest soot particle [81]. The Smoluchowski equation describes the interaction of two PAHs of the same type as is the case in particle inception. The transient particle number for each size class, i , is described by Equation 3.1. The equation consists of a particle-producing term and a particle-consuming term. Particles of size class i are produced when two particles of smaller size, class $i - k, 0 < k \leq i$, merge. Particles of larger size class $i + k, 0 \leq k < N - i$, are produced by consuming particles of size class i .

$$\dot{N}_i = \underbrace{\frac{1}{2} \sum_{j=1}^{i-1} (\beta_{j,i-j} N_j N_{i-j})}_{\text{Production of particles}} - \underbrace{\sum_{j=1}^{\infty} (\beta_{j,i} N_i N_j)}_{\text{Consumption of particles}} \quad (3.1)$$

The frequency factor $\beta_{j,i-j}$ is a probability weight for the production of particles of size class i by particles of size class j and $i-j$. Factor $\beta_{i,j}$ is a probability weight for the consumption of particles of size class i by particles of size class

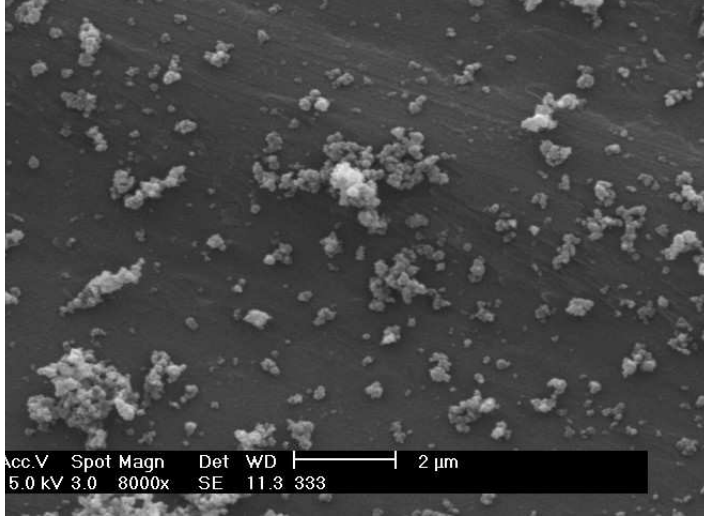


Figure 3.1: Soot particles in wood chips pyrolysis (electron microscope) [82].

j and i . The frequency factor is given by:

$$\beta_{i,j} = \epsilon_{ij} \sqrt{\frac{8\pi k_B T}{\mu_{i,j}}} (r_i + r_j)^2 \quad (3.2)$$

where k_B is the Stefan Boltzmann constant, $\mu_{i,j}$ the reduced mass, r_i the radius of particles in class i and finally ϵ_{ij} is the size-dependent Van der Waals enhancement factor due to either the attractive or repulsive forces between the particles. However, this section deals with the inception of particles which is a growth process. Therefore, only the production of particles in class i is considered:

$$\dot{N}_{i,pi} = \frac{1}{2} \sum_{j=1}^{i-1} (\beta_{j,i-j} N_j N_{i-j}) \quad (3.3)$$

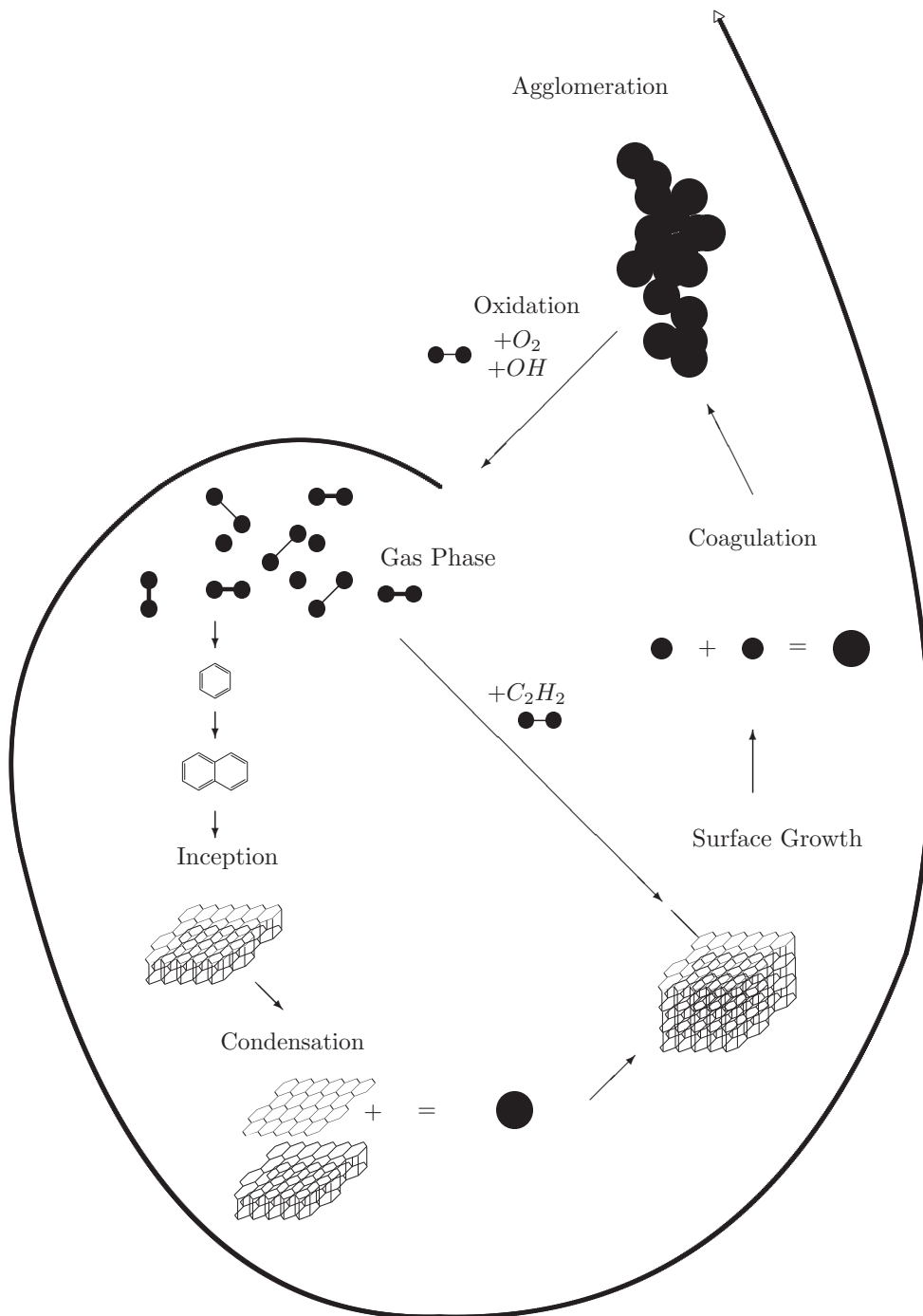


Figure 3.2: Process of soot formation.

3.2.1 Modeling particles inception

Frenklach et al. [64] suggested replacing the Smoluchowsky equation for all particle size classes by the statistical method of moments of size distribution for the particles. Multiplying equation 3.3 by i^r and summing over all size classes results in the following formulation of the PAH size distribution.

$${}^s\dot{M}_{r,pi} = \frac{1}{2} \sum_{i=1}^{\infty} \sum_{j=1}^{\infty} ((i+j)^r \beta_{i,j} {}^P N_i {}^P N_j) \quad (3.4)$$

The well-known relation between particle volume, V_i , particle mass, m_i , and soot density, ρ_S :

$$V_i = \frac{m_i}{\rho_S} = i \frac{m_1}{\rho_S}$$

leads to the following definition of the frequency factor:

$$\beta_{i,j} = C \cdot \sqrt{\frac{i+j}{ij}} (i^{1/3} + j^{1/3})^2 \quad (3.5)$$

where:

$$C = \epsilon_{i,j} \sqrt{\frac{6k_B T}{\rho_S}} \left(\frac{3m_1}{4\pi\rho_S} \right)^{1/6} \quad (3.6)$$

Kennedy et al. [84] set the Van der Waals enhancement factor for particle inception, condensation and coagulation, $\epsilon_{i,j} = 2.2$, which leads to the C factor given below.

$$C = 2.2 \cdot \sqrt{\frac{6k_B T}{\rho_S}} \left(\frac{3m_1}{4\pi\rho_S} \right)^{1/6} \quad (3.7)$$

The PAHs involved in particle inception are assumed to be members of the same size class $i = j$, based on the smallest unit, carbon monomers. This leads to the following frequency factor.

$$\beta_{i,j} = \sqrt{32} \cdot C \cdot i^{1/6} \quad (3.8)$$

The source terms for the moments with respect to particle inception can be formulated as a function of the moments for the soot particle and PAH size distribution. P denotes the PAH distribution:

$${}^s\dot{M}_{r,pi} = \frac{1}{2} C \sum_{k=0}^r \binom{r}{k} ({}^P M_{k+\frac{1}{6}} {}^P M_{r-k}) \quad (3.9)$$

The moments ${}^P M_0 - {}^P M_r$ result in the fast polymerization model for PAH growth. Moments of fractional order are obtained by Lagrange interpolation.

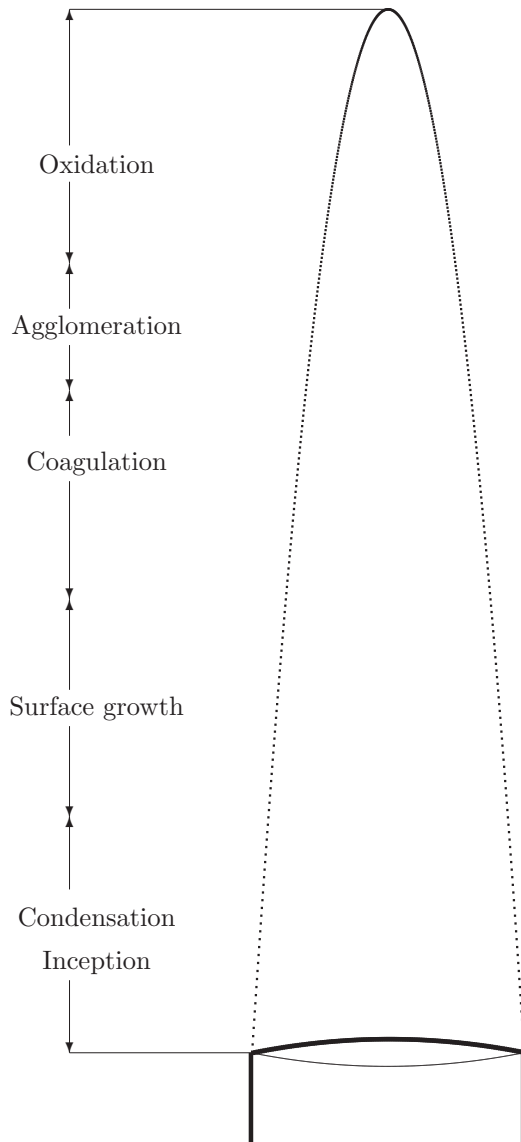


Figure 3.3: A schematic description of the dominant sources of soot formation in different zones in a flame. The radial components are neglected, after Megaridis and Dobbins [83].

3.3 Condensation

Condensation is the process in which one two-dimensional PAH join onto a three-dimensional soot particle. As for particle inception, the Smoluchowsky equation is used to describe this process.

$$\dot{N}_{i,con} = \underbrace{\sum_{j=1}^{i-1} (\beta_{j,i-j} {}^P N_j {}^S N_{i-j})}_{\text{Production term}} - \underbrace{\sum_{j=1}^{\infty} (\beta_{j,i} {}^S N_i {}^P N_j)}_{\text{Consumption term}} \quad (3.10)$$

3.3.1 Modeling condensation

$${}^S \dot{M}_{i,con} = \sum_{i=1}^{\infty} \sum_{j=1}^{\infty} (i+j)^r \beta_{j,i} {}^P N_j {}^S N_{i-j} - \sum_{i=1}^{\infty} \sum_{j=1}^{\infty} (i^r \beta_{j,i} {}^S N_i {}^P N_j) \quad (3.11)$$

Condensation describes the interactions between particles of different size classes. Assuming that one of the particles is much larger than the other ($i \gg j$) the collision frequency is given by:

$$\beta_{i,j} = C j^{-\frac{1}{2}} i^{\frac{2}{3}} \quad (3.12)$$

The resulting source terms for the moments with respect to condensation can be formulated as a function of the moments for the soot particle and PAH size distribution.

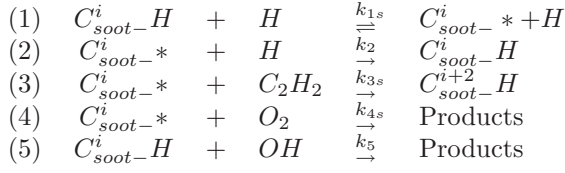
$${}^S \dot{M}_{r,con} = C \sum_{k=0}^{r-1} \binom{r}{k} ({}^P M_{k+\frac{1}{6}}^P M_{r-k}) \quad (3.13)$$

3.4 Surface growth

The particle grows via reactions with the gas phase. Acetylene (C_2H_2) is mainly responsible for the growth of soot particles.

Surface growth and oxidation are heterogeneous reactions in which the soot particles interact with the gas phase to either gain or reduce mass. Different approaches have been undertaken to define the rate of surface growth. The models are based on the assumption that the rate of surface growth is dependent on either the soot volume fraction, or on the surface area of the soot particles. In the latter case the fractal dimension of the surface is of relevance. Wagner [85] gave an empirical expression of the rate of surface growth as a function of soot volume fraction, f_v :

$$\frac{df_v}{dt} = k(f_{v,\infty} - f_v) \quad (3.14)$$

Table 3.1: The HACA-mechanism

where k is the empirical rate constant for the surface reactions and $f_{v,\infty}$ is the final value of the soot volume fraction. A model based on the soot surface has been presented by Harries and Weiner [49]. This empirical formulation of the rate of surface growth was found to be:

$$\rho \frac{df_v}{dt} = k_S S [C_2H_2] \quad (3.15)$$

where k_S is the empirical rate constant for the surface reactions, S is the surface area of the soot particle and ρ the soot density. It was shown that the rate of surface growth decreases with increasing size of the particle, which coincides with the age of the particle. A chemical reaction path for the surface reactions has been given by Frenklach and Wang [86]. The principle of active sites on soot particles was introduced in this context. The active site parameter indicates the reaction activity of the soot surface and allows the particle to take part in the gas phase reactions. An active site on the surface of the soot particle is a C atom, bound to a hydrogen radical, namely the atom C_{soot-H}^i and the radical active site C_{soot-*}^i . The surface reaction constants are then obtained from the PAH reactions. The growth rate can be formulated as follows.

$$\rho \frac{df_v}{dt} = k_3 [C_2H_2] [C_{soot-*}^i] \quad (3.16)$$

Surface growth changes with time. The surface reactions *old* soot particles differs from the reactivity of *young* particles. This phenomenon is topic of a number of studies, which are discussed in chapter 5.

3.5 Coagulation

Two soot particles merge. The process coagulation is a process of growth. Coagulation is the merging of two spherical particle into one larger spherical particle. The number density decreases in this process while the soot volume fraction remains constant. When describing coagulation, three different cases

need to be considered. They are coupled to the "crowdedness" of the space, which is expressed by the Knudsen number:

$$Kn = \frac{2\lambda}{d} \quad (3.17)$$

d is the diameter of the particles, and λ is the mean free path.

1. ($Kn \gg 1$) the free molecular regime: the path between the particles is much larger than the particle diameter. The particles in this regime are free to move around. The regime consists of a continuum flow.
2. ($0.1 < Kn < 10$) the transition regime: is the state between the free molecular and the continuum regime.
3. ($Kn \ll 1$) the continuum regime: the path between the particles is much smaller than the particle diameter. The regime is quite crowded.

However, the Smoluchowski equation is valid in all three regimes with a collision frequencies adjusted to the crowdedness of the regime:

$$\dot{N}_{i,coag} = \frac{1}{2} \sum_{j=1}^{i-1} (\beta_{j,i-j} \mathbf{s} N_j \mathbf{s} N_{i-j}) - \sum_{j=1}^{\infty} (\beta_{j,i} \mathbf{s} N_i \mathbf{s} N_j) \quad (3.18)$$

More details and different approaches for the calculation of this process are discussed in chapter 5.

3.6 Agglomeration

Large clusters of particles are build. After having reached a critical diameter d_c , soot particles join and built agglomerates, larger chainlike soot structures. Agglomerates are clusters of at least two primary particles. Soot particles denominate primary particles as well as agglomerates. The number density of primary particles remains constant when agglomerates are formed. Agglomerates differ in shape and size. The individual formation of those particles has not yet been subject of models. A large number of experimental studies measuring parameters describing shape and size of agglomerates, have been undertaken since the eighties [87, 88, 89, 90, 91]. Frenklach and Kazakov [92] made the first attempt to include this process into their existing model applying the method of moments described in section 5.2. Agglomeration also changes with time Faeth et al. [93] and is therefore topic of chapter 5.

3.7 Oxidation

The soot particle loses mass in reactions with gas phase molecules O_2 and OH . Soot particles grow through particle inception, surface growth and coagulation processes and reduce through oxidation processes.

Chapter 4

Soot models

A large number of models have been developed to describe the formation of soot in various combustion situations. These approaches contain varying chemical models, ranging from simple chemical mechanisms with a few reactions to large detailed chemical models. They also vary in the description of soot formation and the postprocessing or interacting flow models. Kennedy [94] classified existing models into three groups, a classification which will be followed in this section.

1. Empirical models base completely on experimental data.
2. Semi-empirical computer models contain a mathematical description completed with data originating from experimental results.
3. Detailed models seek to solve the rate equations for elementary reactions that lead to soot.

4.1 Empirical models

The pioneers of the field developed empirical models. Some scientists still work with empirical models since they give a fast result. They base on experimental results and are designed to feature a certain combustion situation and do not describe combustion processes in general. Empirical models do not require complex modelling and are thereby cheap in developing- and CPU time. Most empirical models base on the definition threshold sooting index (TSI). The first to define the TSI as a function of the equivalence ratio were Calcote and Manos [95].

$$TSI = a + b\Phi_C \quad (4.1)$$

a and b are empirical constants and Φ_C is the critical threshold equivalence ratio. The soot formation is expected to begin when the C/O ration exceeds unity. Experiments have shown that this event already occurs at $C/O = 0.5$ [96]. The definition of the TSI was further developed by Gill and Olson [97] who included a contribution of each component of the fuel to the TSI. The model was extended by Glassman and Takahashi [98] who expressed the TSI as a function of an effective equivalence ratio $\Phi \equiv \frac{2C+H}{2O}$. The models were further developed and applied for different combustion conditions. In 1991 Kahn et al. [99] proposed a model describing soot formation in Diesel engines. They assumed that the diameters of soot particles formed in engines was constant for all speeds and loads. As a consequence soot formation was a result of particle inception alone. Particle inception was considered to be a function of pressure, equivalence ratio of unburned gasses and the temperature. Lefebvre [100] applied the Kahn model on gas turbines.

De Ris et al. [101] developed a model describing and applying soot formation in fires in buildings. The method bases on the measurements of the soot layer thickness δ_S , the deposition of soot particles on metal rods placed in different locations in the flame. Megaridis and Dobbins [83] found the soot volume fraction to be proportional to the deposition. Curve fits of the measurements resulted in the following definition of the soot volume fraction:

$$f_V \delta_S = -\lambda_0 \frac{\ln(1 - \epsilon_0)}{7} \quad (4.2)$$

ϵ_0 is the extinction coefficient taken from Markstein [102] and $\lambda_0 \in [0.9, 1.0] \mu m$ is the wavelength. The main interest of this study is to include the radiative properties of the soot into a simple model.

Why is it of interest to spend more time in understanding details in soot formation and oxidation, if such simple models exist? One answer might be the following: In order to be able to counterwork the process of soot formation in combustion and thereby to optimize the combustion as well as to avoid emission and pollution with soot it is not satisfactory to know where soot is build in the flame, but why and how it is generated. Another answer is that it is very exciting to find answers to all the questions asked in this context. Modelers still struggle to achieve the most detailed description of pollution formation in flames, using as little CPU time as possible. The third answer is the applicability of simple models is restricted to the exact conditions of the combustion process. The next two classes of models succeed more and more in describing combustion process in a general way.

4.2 Semi-empirical models

Many semi-empirical models focus on reproducing experimental results on the formation of soot and soot-precursors. They often base on simple chemical models and apply parameters to adjust the theoretical results to experiments. In 1971 Tesner et al. [103], developed a model of soot formation based on simple kinetics and a two step mechanism for the soot production: the formation and reduction of the soot nuclei n . The aim of the model was to interpret measurements performed by Tesner [104] in an acetylene-hydrogen flame.

$$\frac{dn}{dt} = n_0 + (f - g)n - g_0 N n \quad (4.3)$$

where n_0 is the temperature dependent rate of spontaneous generation of nuclei. f and g are branching and terminating coefficients g_0 is the rate loss of nuclei due to collisions with soot particles and N is the number density of soot particles given by:

$$\frac{dN}{dt} = (a - bN)n \quad (4.4)$$

a and b are adjustable parameters. Tesner's soot model can be considered to be the fundament of many following soot models. Some of them will be listed here. The models and experimentalists studied and study soot formation in laminar and turbulent, premixed, co- and counter flow flames.

Surovikin [105] developed a more detailed model to describe the formation of soot particles and added oxidation to the model. Surovikin formulated a model in four steps:

1. Formation of radical nucleus.
2. Growth of nucleus to incipient particle.
3. Growth of incipient particle into carbon particles.
4. Oxidation of the soot particle via O_2 .

Magnussen et al. [106] extended Tesners two step soot concept with the oxidation of soot and coupled it to a simple eddy dissipation model to calculate a turbulent acetylene flame. Here the reactants were assumed to be homogeneously mixed. Brown and Heywood [107] improved the mixing properties by adding a stochastic mixing model to simulate the inhomogeneous mixing and combustion in a diesel engine. Different other flow codes such as the KIVA code were coupled to Tesners two step soot kinetic. Jensen et al. [108] defined a soot model in four steps. The nucleus of soot was considered to be C_2 or C_2H molecules. The four step are as follows:

1. Reversible gas phase mechanism containing 11 reactions, wherein soot nuclei are formed.
2. Coagulation.
3. Soot surface growth.
4. Oxidation.

Graham [109] assumed the first steps of soot formation by the pyrolysis of aromatic hydro carbons. Another model by Dobbins et al. [83] suggested that soot particles were formed in a graphitization process of liquid droplets. Mulholland [87] formulated a simple reaction mechanism for the soot formation process in Arrhenius form where large nuclei were formed in a pyrolysis process of the fuel. The surface growth was assumed to be proportional with soot surface. The fuel itself was considered to be responsible for the surface growth. Kennedy et al. [94] formulated one equation to describe the soot. The number density was assumed to be constant. Moss soot model [110] is of special interest since it bases on the flamelet concept to model soot formation in diffusion flames. The model included several steps to soot formation: particle inception caused an increase in number density. Surface growth, coagulation give their contribution to the process as well as oxidation through O_2 and OH . The source terms for the number density and the soot volume fraction are expressed as functions of temperature and mixture fraction. The model consists of two soot equations for the number density N and the soot volume fraction f_V .

$$\frac{d}{dt}\left(\frac{n}{N_0}\right) = \alpha(Z) - \beta(Z)\left(\frac{n}{N_0}\right)^2 \quad (4.5)$$

$$\rho_S \frac{df_V}{dt} = \gamma(Z)n + \delta(Z) \quad (4.6)$$

The source terms α , β , γ and δ for the number density are given by:

$$\alpha = C_\alpha \rho^2 \sqrt{T} X_{fuel} \exp\left(-\frac{T_\alpha}{T}\right) = \frac{\delta}{144} \quad (4.7)$$

$$\beta = C_\beta \sqrt{T} \quad (4.8)$$

$$\gamma = C_\gamma \sqrt{T} X_C \exp\left(-\frac{T_\alpha}{T}\right) \quad (4.9)$$

where n_0 is the rate of spontaneous generation of nuclei, N is the number density of soot particles, T is the temperature and T_i is the activation temperature. X_{fuel} is the mole fraction of the fuel. C_α , C_β and C_δ are parameters

taken to adjust the model to experiments performed by Moss and Young [111] in ethylene-air flames. Syed et al [112] coupled the model to a parabolic $k - \epsilon$ turbulence model. Another approach was made by Lindstedt [113, 114]. Lindstedt developed soot models for laminar and turbulent diffusion flames. He also applied the flamelet approach to compute species concentrations and a simple soot model to predict soot volume fractions in diffusion flames. The flamelet model was coupled to a CFD code. He made the crucial contribution to the model evolution by making C_2H_2 responsible for the nucleation process.



The effect of acetylene on soot formation is meanwhile well studied phenomenon [115]. The Lindstedt model contains the usual steps: Surface growth, oxidation nucleation and coagulation and a few chemical reactions for the gas phase. The result is adjusted to experiments by parameter variations. A number of modelers are occupied with studying the reduction of soot, since this is a very relevant phenomenon. Among those are Kennedy [84], who formulated a simple OH , O_2 oxidation mechanism containing the enduct CO_2 , Nagel-Strickland-Constable [116] formula correct formulation of O_2 -oxidation was applied by Kennedy. Mechanisms for different fuels and species were defined such as a methane mechanism by Smooke et al. [117] and a mechanism involving C_2 chemistry by Frenklach. The mechanism grew larger time being together with an increasing number of reactants involved. Numerical methods were needed and developed in order to solve nonlinear differential equations balancing the chemistry. Another contribution to the field comes from Kollmann et al. [118]. A PDF-transport model was used to simulate the reacting turbulent flow in a sooting ethylene diffusion flame. Kollmann et al. calculated the process of soot formation using a simple soot model based on experimental chemical sources terms [118]. In this approach the sources terms are functions of mixture fraction.

A simplified soot formation model for the two fuels propylene (C_3H_6O) and plexiglas or methylmethacrylate $CH_2 : C(CH_3)COOCH_3$ was developed and validated by Moss and Steward [119]. Those materials were chosen because of their relevance in compartment fires. The average particle diameter is given by:

$$d_p = \left(\frac{6f_v}{n\pi}\right)^{1/3} \quad (4.11)$$

the rate of soot volume fraction is defined in terms of nucleation and surface growth

$$\frac{d}{dt}(\rho_s f_v) = \gamma n + 144 \cdot \alpha \quad (4.12)$$

where γn is the surface growth controlled by the rate expression:

$$\gamma = C_\gamma \rho \sqrt{T} \chi_c \exp \frac{T_\gamma}{T} \quad (4.13)$$

and $144 \cdot \alpha$ the nucleation, controlled by the rate expression:

$$\alpha = C_\alpha \rho^2 \sqrt{T} \chi_c \exp \frac{T_\alpha}{T} \quad (4.14)$$

The rate of number density is defined in terms of nucleation and coagulation:

$$\alpha - \beta \left(\frac{n}{N_0} \right)^2 \quad (4.15)$$

where the coagulation is determined by the Smoluchowsky expression and

$$\beta = C_\beta \sqrt{T} \quad (4.16)$$

From experiments with other fuels the following activation temperatures have been observed: $T_\alpha = 46100K$ $T_\gamma = 12600K$. C_α , C_β and C_γ are empirical.

4.3 Detailed chemical models

In order to give answers that are generally valid for any combustion condition modelers have began to work on models which are free of experimental input parameters. Experiments serve for validation in this context. The models seek to define mechanisms and for the complete process and increase understanding of the formation of soot and soot precursors such as C_2H_2 and PAH's. One of the biggest contributions in this field comes from Frenklach and coworkers.

Chapter 5

Aging

The definition of the terms *old* and *aging* varies with interpreter, even valid in the field of soot formation. The combustion society does not agree in the definition of when a soot particle can be considered *old*. The understanding differs in terms of timescale, particle size and shape as well as temperature range. Hence, the processes considered when talking about aging also differ. The group dealing with simple fuels (which mostly apply to engines and turbines) consider a change in the surface reactivity. Here a *young* particle is about 15 nm and on *old* particle about 30 nm [120]. Here aging happens within a timescale of ms. The group dealing with fires considers all processes which happen when the particle leave the flame. At this stage the processes of oxidation and nucleation are terminated. The particles are subjected to growth, mostly via coagulation. The particles increase in fractality [121]. The temperature are relative lower. The group of scientists which are interested in atmospheric phenomenon consider particles, which are several days old. The discussion in this report tries to satisfy all groups. Hence, the different scientific results on the processes of surface growth, coagulation and agglomeration (section 4 and figure 3.2) are analyzed. A summary of the work reported in literature will be summarized and analyzed in the following sections. The chapter terminates by referring a study on aging of smoke from large fires, which considers times up to 44 h.

5.1 Surface growth

Aging alters the process of surface growth of soot particles [122]. It is realized through a fall off on specific growth rates observed in laboratory flames. In spite

the fact that this has been known since 1973 [123] there are later models such as the model by Colket and Hall [124], which ignore the phenomenon in order to simplify the model. Another reason for ignoring the phenomenon in the model open question concerning the process. Most studies on surface growth have been made in premixed flames.

Wersborg studied the process of carbon formation in a premixed acetylene-oxygen flame in 1973. Those studies were among the first to describe the change in alteration in surface growth. "Surface growth may cause a trend toward a more uniform distribution by the faster growth of smaller particles." If the

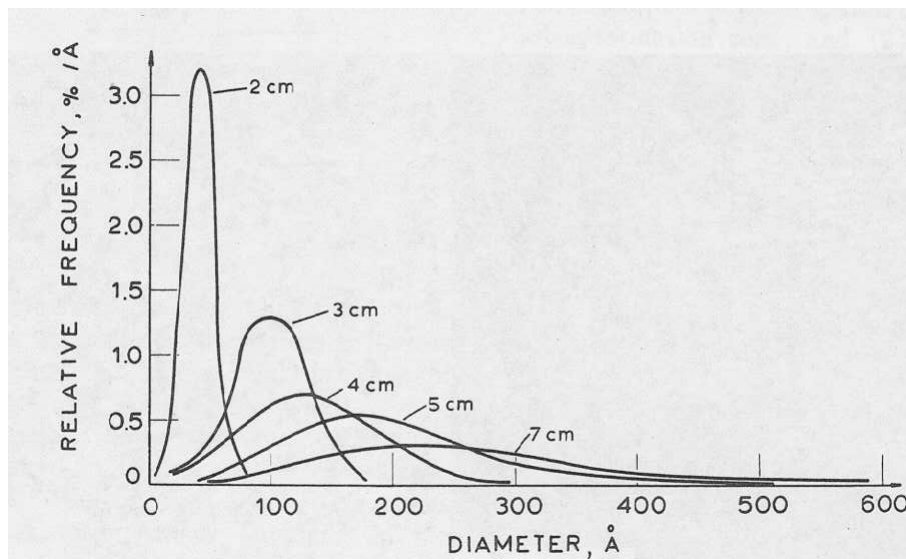


Figure 5.1: Particle diameter distributions at different heights above the burner [123].

nuclei are assumed to grow by surface growth alone, their appearance size can be estimated from the observed surface growth rate and the to the sampling positions first encountered. Wersborg's research are presented in figures 5.1,5.2. The figures show the decrease of the mean particle diameter with travel time 5.1, the stagnation in volume growth with height over the burner 5.2(a) and finally the change in change in surface growth 5.2 (b).

5.1.1 Constant surface reactivity

Harris and Weiner [125] declared surface growth mainly responsible for the mass of the soot ultimately formed in the combustion process. The increased mass growth rate found in richer flames is accounted for by the increased surface area available due to particle inception rather than by a much higher amount of growth species. Hence, particle inception controls the amount of soot formed in the flame even though the process does not primarily contribute to any mass. The main species of growth is acetylene with diacetylene as a minor species [120].

Harris and Weiner [126] received reasonable results in assuming a constant surface growth rate depending on acetylene. They found only a weak temperate dependency.

$$k_{C_2H_2}^0 = 1.8 \times 10^3 \quad (5.1)$$

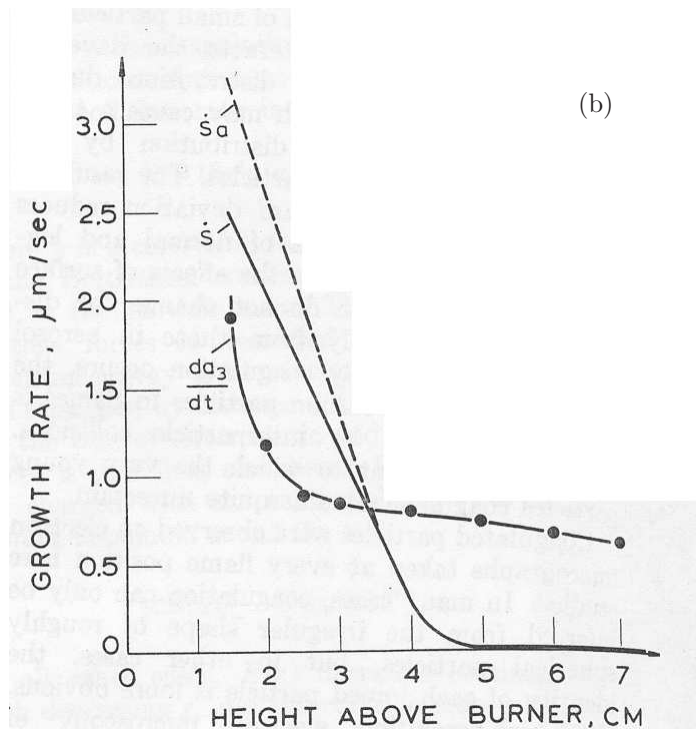
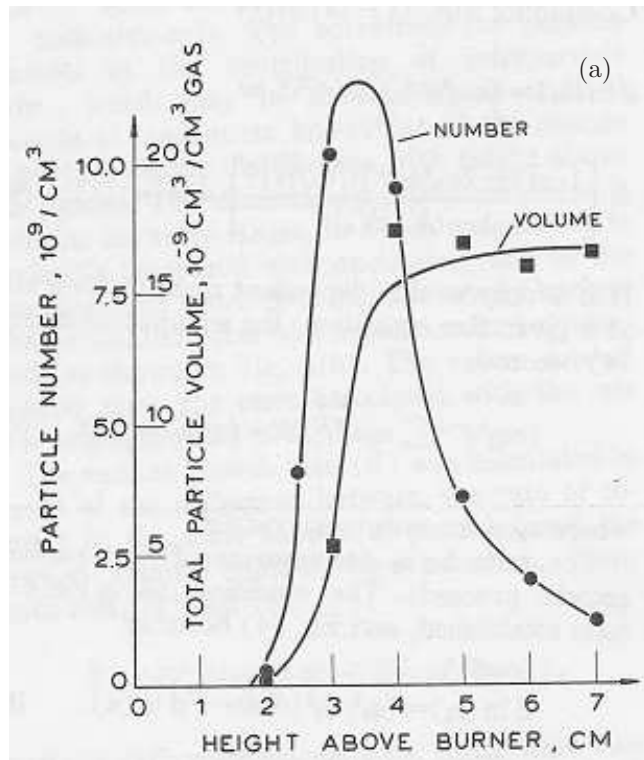


Figure 5.2: (a) Particle number concentration and total particle volume per unit volume gas [123]. (b) Rate of change of volume mean radius $\frac{da_3}{dt}$ and surface growth rate \dot{S} . The dashed line (\dot{S}_a) represents \dot{S} plus the surface growth equivalent of volume addition by nucleation [123].

5.1.2 Temperature dependence of the active site parameter

1985 Dasch [122] presented kinetic models introducing the decay of the surface reactivity, also called the active site parameter α , leading to a solution of the Smoluchowsky [127] equation of:

$$\dot{f}_v = 3(4\pi N f_v^{2/3})^{1/3} k_s^0 e^{-\alpha t} \quad (5.2)$$

where:

$$\alpha = 3.5 \times 10^7 \exp\left(\frac{-45 \text{ kcal}}{RT}\right) s^{-1} \quad (5.3)$$

The next definition of the active site parameter was made by Appel et al. [128]. The concentration of the active radical sites, C_{soot}^* , and $C_{soot}^* C_2H_2$, is found, as mentioned previously, based on the assumption of a quasi-stationary state:

$$[C_{soot}^*] = \sum_{i=1}^{\infty} \alpha \frac{\chi_{soot}^*}{N_A} S_i N_i \quad (5.4)$$

where S_i is the surface area and N_i the number density of particles of size class i . α is the fraction of the active sites available for chemical reactions. α is a steric factor, that accounts for the probability of the gaseous species colliding with the reactive prismatic planes of a soot particle [129]. It was found to quantify the temperature dependent morphology of the soot particles [128]. Appel et al. [128] developed a temperature formulation of the active site parameter for premixed flames:

$$\alpha = \tanh\left(\frac{a}{\log \mu_1} + b\right) \quad (5.5)$$

where μ_1 is the first size moment of the soot particle distribution, and a and b are fitted parameters given by:

$$a = 12.65 - 56.3 \cdot 10^{-4} \cdot T \quad (5.6)$$

and:

$$b = -1.38 + 6.8 \cdot 10^{-4} \cdot T \quad (5.7)$$

As mentioned above, the surface annealing of aging soot particles is a result of a decreasing H atom concentration and the ensuring reduction in radical sites [86]. Frenklach and Wang [86] claimed that α must decrease with temperature. They argued that at high temperatures soot particle crystallites align themselves in such a way that the active sites of neighbouring crystallites face each

other, and thereby thus the access of gaseous species. Each benzene molecule contained in a soot particle is assumed to have one active site, $\chi_{soot}S_1$, which results in the following expression for the active sites:

$$\chi_{soot}S_i = \chi_{soot}S_1 i^{2/3} = i^{2/3}, \quad (5.8)$$

where i is the size class of the molecule. The source terms of surface growth and oxidation for the soot moments follow the formulation of Balthasar [53]:

$${}^S\dot{M}_{0,sg} = 0 \quad (5.9)$$

$${}^S\dot{M}_{r,sg} = \alpha k_{3a,f} [C_2H_2] f_{3a} A \cdot \sum_{k=0}^{r-1} \binom{r}{k} M_{k+\frac{2}{3}} 2^{r-k}, \quad r = 1, 2, \dots \quad (5.10)$$

and for oxidation:

$${}^S\dot{M}_{0,ox} = -\alpha(k_{4a}[O_2]A + k_5[OH])N_x \quad (5.11)$$

$${}^S\dot{M}_{r,ox} = \alpha(k_{4a}[O_2]A + k_5[OH]) \cdot \sum_{k=0}^{r-1} \binom{r}{k} M_{k+\frac{2}{3}} (-2)^{r-k}, \quad r = 1, 2, \dots \quad (5.12)$$

where:

$$A = \frac{k_{1a,f}[H] + k_{1b,f}[H] + k_5[OH]}{k_{1a,b}[H_2] + k_{1b,b}[H_2O] + k_2[H] + k_{3a,f}[C_2H_2] + k_{4b}[O_2]} \quad (5.13)$$

In order to achieve closure of the system the number density of the smallest size class must be known. Hence, the probability of the burn-out of the soot particles is assumed to be proportional to the mean particle size. This results in a rate of oxidation for the zeroth moment:

$${}^S\dot{M}_{0,ox} = -(k_{4a}[O_2]A + k_5[OH]){}^SM_{-\frac{1}{3}} \quad (5.14)$$

5.1.3 Influence of the surface reactivity on soot formation in diffusion flames

Most recent studies on surface growth in diffusion flames assume constant active site parameter. Feath et al. [93] assumes in their study on surface growth the parameter to be unity for both premixed and non-premixed flames. Dederichs [2] presented a study on how the soot formation in a laminar and a turbulent diffusion flame are affected by the change in active site parameter.

Laminar diffusion flame

The process of soot surface growth was previously discussed for turbulent diffusion flames, in section 5.1.4. This section deals with the effects on laminar acetylene/nitrogen/air flames.

Soot surface growth dependence

The questions of whether the growth of the soot surface can be modelled as a function of soot volume fraction [85], the soot surface itself [120] or the number density is posed in this section. The focus of this section is to study the effect of the previously described surface effects on laminar diffusion flames using the unsteady flamelet approach.

The mean soot volume fraction is modelled using the unsteady flamelet model describing the laminar acetylene/nitrogen/air flame described above. The active site parameter was set to 0.25 and two moments were considered. The results are compared with the experimental data of Xu and Feath [130]. As in Section 5.1.4, the models are based on the following assumption:

1. Soot surface growth is a function of the soot surface.
2. soot surface growth is a function of the number density.
3. soot surface growth is a function of the soot diameter to the power of 2.25.

Figure 5.3 (i) presents the mean soot volume fraction in axial direction. The maximum of soot volume fraction for the models based on the three assumptions coincide in space have the same order of magnitude. The soot volume fraction is still underestimated when assuming the surface growth to be a function of number density. The profiles predicted by the model assuming that the surface growth is a function of the soot surface are close to those predicted by the model assuming the surface growth is a function of $d^{2.25}$. Both profiles agree reasonably with experimental data.

Active sites

Figure 5.3 shows three values of the active site parameter. The reference value of the parameter of $0.25 \pm 14\%$. The parameter is by a factor 0.7 lower than the parameter applied by Frenklach and Wang [129] for a laminar premixed $C_2H_2/O_2/Ar$ flame at pressures of 12 kPa. The soot volume fraction was assumed to depend on the surface area of the soot particles. The soot volume fraction changes by 8% when varying the activity of the site by 14%. It can

be concluded that the active site parameter influences the formation of soot in laminar diffusion flames. The effect is not as large as for turbulent flames. This is due to the fact that the flame is laminar and the turbulent mixing, which supplies the particle in radicals does not affect the process. The active site parameter decreases with the absence of radicals [96].

5.1.4 Turbulent diffusion flame

In spite the fact, that the process has been the subject of many studies (see Haynes and Wagner [96]), many questions remain unanswered.

In the following the unsteady flamelet model considering two moments will be applied to study the in on-axis soot volume fraction depends on the active site parameter. The results will be compared with experiments by Young et al. [131].

Soot surface growth dependence

One of the questions still not answered is whether the growth of the soot surface can be modelled as a function of soot volume fraction (as claimed by Wagner et al. [85]), the soot surface itself (as postulated by Harris et al. [120]) or the number density as discussed previously.

The mean soot volume fraction is modelled using the unsteady flamelet model describing the turbulent ethylene/air flame described earlier. The active site parameter applied was 0.7, and the calculations were performed using two moments. The model is based on the following assumptions:

1. Soot surface growth is a function of the soot surface area.
2. Soot surface growth is a function of the number density of soot particles.
3. Soot surface growth is a function of the soot particle diameter raised to the power of 2.25.

Figure 5.4 (i) presents the axial mean soot volume fraction. Model modifications based on the three assumptions peak at the same point in space for all three models. The soot volume fraction is badly underestimated when assuming the surface growth to be a function of number density. This under-prediction is unaffected by the active site parameter, which is the subject of the next section. The result in best agreement with the experimental profile is that assuming the assuming the surface growth is a function of soot particle surface area.

Active sites

The active site parameter is another variable of interest. It describes the reactivity of the soot surface. The effect of a change in this parameter on soot volume fraction is illustrated in this section. The model applied is the unsteady flamelet model considering two moments. The surface growth is assumed to depend on the soot particle surface area.

Figure 5.4 shows three values of active site parameter assuming an reference active site parameter of $0.7 \pm 14\%$. The soot volume fraction changes by 30% when varying the activity of the site. It can be concluded that the active site parameter has considerable influence on the formation of soot in turbulent diffusion flames.

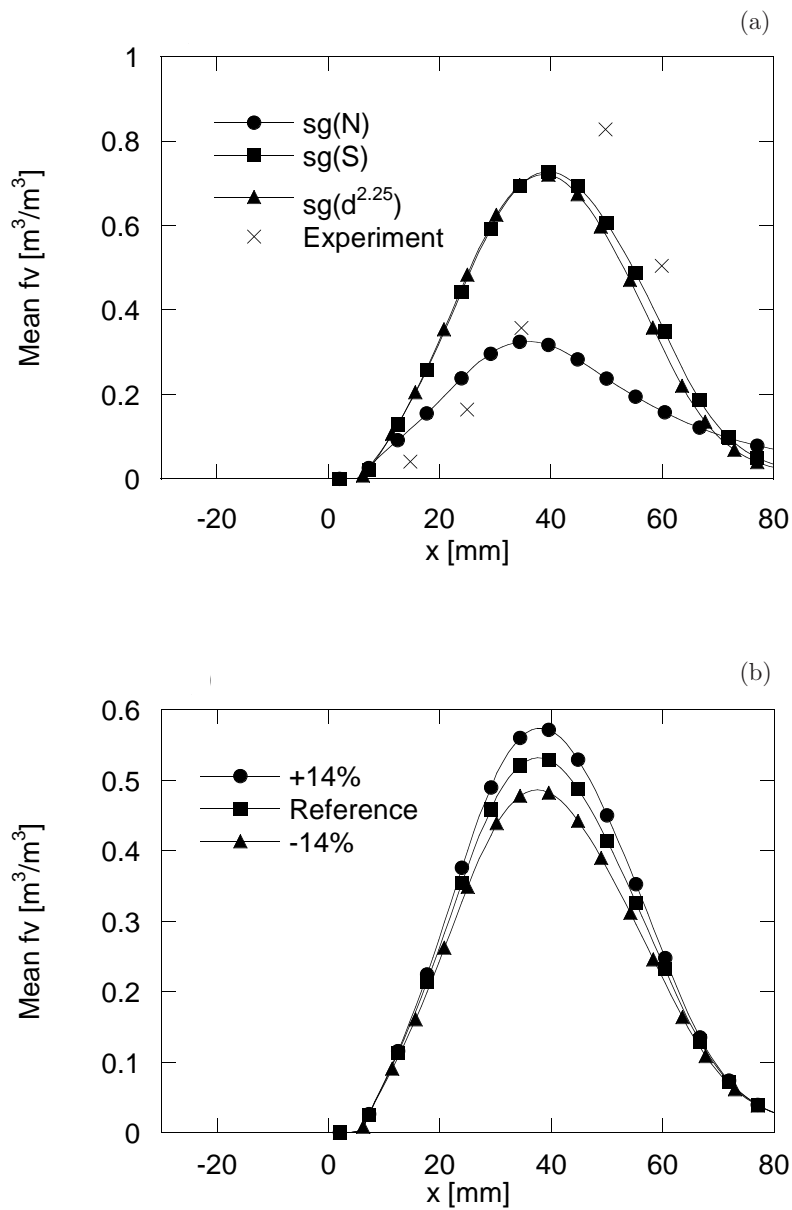


Figure 5.3: (a) The dependence of the surface growth on the soot number density (\bullet), the soot surface (\blacksquare) and the diameter $d^{2.25}$ (\blacktriangle). (b) Mean soot volume fraction as a function of the active site parameter, increased (\circ) and decreased (\blacksquare) by 14%. The experimental data are from Xu and Faeth [130].

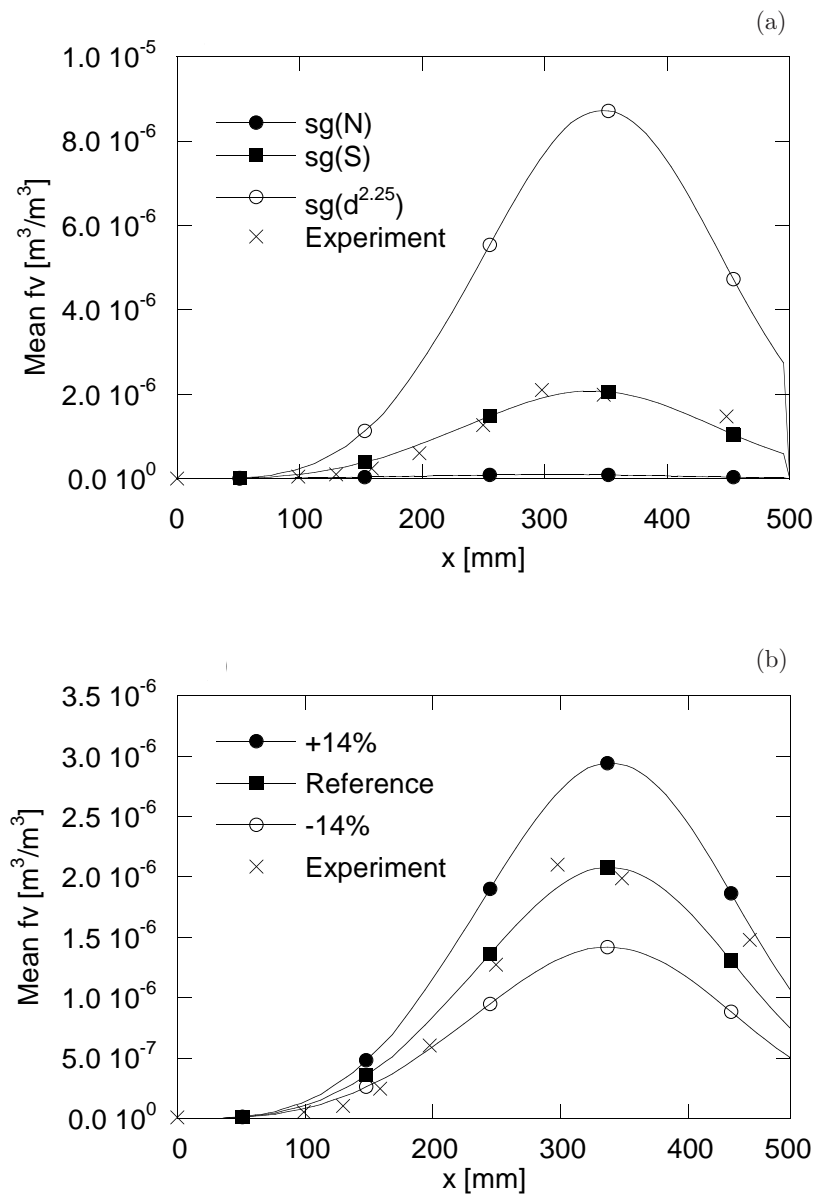


Figure 5.4: (a) The dependence of surface growth on the soot number density (\bullet), the soot surface (\blacksquare) and the diameter $d^{2.25}$ (\circ). (b) Mean soot volume fraction as a function of the active site parameter, increased (\circ) and decreased (\blacksquare) by 14%. The results are compared with experiments by Young et al. [131].

5.2 Methods of moments

5.2.1 Coagulation

Coagulation is a process of growth. Coagulation is the merging of two spherical particles into one larger spherical particle. The number density decreases in this process while the soot volume fraction remains constant. When describing coagulation, three different cases need to be considered. However, the Smoluchowski equation is valid in all three regimes with a collision frequencies adjusted to the crowdedness of the regime. The coagulation as a of moments of the soot particle size distribution:

$$\mathbf{S}\dot{M}_{i,coag} = \sum_{i=1}^{\infty} \sum_{j=1}^{\infty} ((i+j)^r \beta_{j,i} \mathbf{S}N_j \mathbf{S}N_{i-j}) - \sum_{i=1}^{\infty} \sum_{j=1}^{\infty} (i^r \beta_{i,j} \mathbf{S}N_i \mathbf{S}N_j) \quad (5.15)$$

Coagulation in the free molecular regime.

The Knudsen number in this regime is $Kn \gg 1$ and the particles are free to move. The particle size ranges from $i = 0$ to $i = \infty$. The collision frequency in this regime is given by equation (3.7) and:

$$\beta_{i,j} = Cj^{-\frac{1}{2}}i^{\frac{2}{3}} \quad (5.16)$$

In order to obtain closure, Frenklach et al [64] introduced function $\langle \Phi_{x,y} \rangle$ and reformulated the source terms of the coagulation for the soot moments:

$$\mathbf{S}\dot{M}_{r,coag} = \frac{1}{2} \sum_{k=1}^{r-1} \binom{r}{k} \langle \Phi_{x,y} \rangle \mathbf{S}M_0^2 \quad (5.17)$$

where

$$\langle \Phi_{x,y} \rangle = C \langle f_{x,y} \rangle \quad (5.18)$$

where $\langle f_{x,y} \rangle$ is obtained by $f_{x,y}$ through the following relation:

$$f_{x,y} = \sum_{i=1}^{\infty} \sum_{j=1}^{\infty} (i+j)^r \frac{(i^{\frac{1}{3}} + j^{\frac{1}{3}})^2}{\sqrt{ij}} i^x j^y n_i n_j \quad (5.19)$$

where $n_i = \frac{N_i}{\mathbf{S}M_0}$ is the fraction of particles of size class i related to the sum of all particles. The value of $\langle f_{x,y} \rangle$ is determined by Lagrange interpolation between the logarithms of ${}^0f_{x,y}, {}^1f_{x,y}, {}^2f_{x,y}, \dots, {}^rf_{x,y}$ can even be an expression of the moment formulation [53]

$$\begin{aligned} {}^rf_{x,y} = & \mu_{(k+x+\frac{1}{6})} \mu_{(r+y-k-\frac{1}{2})} + 2\mu_{(k+x-\frac{1}{6})} \mu_{(r+y-k-\frac{1}{6})} \\ & + \mu_{(k+x-\frac{1}{2})} \mu_{(r+y-k+\frac{1}{6})} \end{aligned} \quad (5.20)$$

The fractional moments $\mu_r = \frac{\mathbf{s}M_r}{\mathbf{s}M_0}$. Lagrange interpolation is used to obtain the fractional moments and the expression of $r f_{x,y}$.

Coagulation in the continuum regime.

The Knudsen number in this regime is $Kn \ll 1$ and we deal with a continuous flow. The collision frequency in this regime is given by equation :

$$\beta_{ij}^c = K \left(\frac{C_i}{i^{\frac{1}{3}}} + \frac{C_j}{j^{\frac{1}{3}}} \right) (i^{\frac{1}{3}} + j^{\frac{1}{3}}) \quad (5.21)$$

c denotes the continuum regime and

$$K = \frac{2k_B T}{3\eta} \quad (5.22)$$

where η is the viscosity of the gas and the Cunningham slip correction factor C_i is given by:

$$C_i = 1 + 1.257Kn(i) \quad (5.23)$$

Van der Waals forces are small in this regime [132], which is the reason why no enhancement factor is included. The source terms for the coagulation of soot particles in terms of the moments are give by:

$$\begin{aligned} \mathbf{s}M_{0,coag}^c &= \frac{1}{2}K \sum_{k=1}^{r-1} \binom{r}{k} \cdot \left[2 \mathbf{s}M_k \mathbf{s}M_{(r-k)} \right. \\ &+ \mathbf{s}M_{(k+\frac{1}{3})} \mathbf{s}M_{(r-k-\frac{1}{3})} + \mathbf{s}M_{(k-\frac{1}{3})} \mathbf{s}M_{(r-k+\frac{1}{3})} \\ &+ 2.514\lambda \left(\frac{\pi\rho_s}{6m_1} \right)^{\frac{1}{3}} \cdot \left(\mathbf{s}M_{(k-\frac{1}{3})} \mathbf{s}M_{(r-k)} \right. \\ &+ \mathbf{s}M_{(k)} \mathbf{s}M_{(r-k-\frac{1}{3})} + \mathbf{s}M_{(k+\frac{1}{3})} \mathbf{s}M_{(r-k-\frac{2}{3})} \\ &\left. \left. + \mathbf{s}M_{(k-\frac{2}{3})} \mathbf{s}M_{(r-k+\frac{1}{3})} \right) \right] \end{aligned} \quad (5.24)$$

Coagulation in the transition regime.

The Knudsen number in this regime is $(0.1 < Kn < 10)$. This state between the free molecular and the continuum regime. The semi empirical formula of Fuchs [133] was developed to describe the coagulation in the transient regime.

$$\tilde{\beta}_{ij} = \tilde{\beta}_{ij}^c \left[\frac{\frac{1}{Kn(i)} + \frac{1}{Kn(j)}}{\frac{1}{Kn(i)} + \frac{1}{Kn(j)} + 2\sqrt{\tilde{\delta}_i^2 + \tilde{\delta}_j^2}} + \zeta \frac{\tilde{\beta}_{ij}^c}{\tilde{\beta}_{ij}^f} \right]^{-1} \quad (5.25)$$

where

$$\begin{aligned}\zeta &= \frac{1}{3} \sqrt{\frac{K\rho}{\lambda\eta}} \\ \tilde{\delta} &= \frac{1}{Kn} \left[\frac{(1 + \frac{\pi}{\zeta C \sqrt{Kn}})^3 - (1 + (\frac{\pi}{\zeta C \sqrt{Kn}})^2)^{3/2}}{3 \left(\frac{\pi}{\zeta C \sqrt{Kn}}\right)^2} - 1 \right] \\ \tilde{\beta}_{ij}^f &= \sqrt{Kn(i)^3 + Kn(j)^3} (Kn(i)^{-1} + Kn(j)^{-1})^2 \\ \tilde{\beta}_{ij}^c &= \sqrt{C_i Kn(i) + C_j Kn(j)} (Kn(i)^{-1} + Kn(j)^{-1})\end{aligned}$$

Partsinis [134] approximated the coagulation rate for particles of the same size by the harmonic mean of the continuum and the free molecular rate. Frenklach [92] first extended the approach to a wide range particle size distribution.

$$\mathbf{S}\dot{M}_{r,coag} = \frac{\mathbf{S}\dot{M}_{r,coag}^f \mathbf{S}\dot{M}_{r,coag}^c}{\mathbf{S}\dot{M}_{r,coag}^f + \mathbf{S}\dot{M}_{r,coag}^c}, \quad r = 0, 2, 3, 4... \quad (5.26)$$

5.2.2 Agglomeration

The method of moments can even be applied to describe the formation of sooty agglomerates. The application was introduced by Frenklach and Kazakov is based on the assumption that agglomerates are composed of spherical equal-sized primary particles. One needs to differentiate the formation of primary particles on one hand and the formation of the agglomerates, an adjunction of primary particles with point contact on the other need to be considered. Agglomerates are subject of soot formation processes such as condensation of PAH's, surface growth and coagulation with other primary particles and other agglomerates as well as soot reduction processes as oxidation via O_2 and OH . The number of primary particles in an agglomerate may be described via its radius of gyration [135], $R_g = \sqrt{\frac{1}{n} \sum_i r_i^2}$, r_i is the distance of the i^{th} primary particle to the center of mass of the aggregate.

$$n = k_f \left(\frac{2R_g}{d_p} \right)^{D_f} \quad (5.27)$$

where n is the number of primary particles in an aggregate, D_f is the fractal or Hausdorff dimension. The fractal dimension was found to be in the range

[1.7;2.07] ([89, 136]). Equation 5.27 was found to be valid if $D_f \geq 2$ or if the aggregates have similar size [92]. Otherwise the collision frequency is overestimated since small particles sometimes pass through large particles without adsorption. k_f , denoted by Mandelbrot [137] as the first order lacunarity or fractal prefactor, is a parameter characterizing the aggregate density and cutoff of fractality. In other words, the lacunarity describes the gaps in the surface of the fractal shape of the agglomerate. d_p denotes the diameter of primary particles:

$$d_p = \left(\frac{6m_1 m}{\pi \rho n} \right)^{1/3} \quad (5.28)$$

Equation 5.27 is strictly only valid for large agglomerates. Dobbins et al [138] showed that the validity of this statistical approach down to small scale agglomerates containing about 5 particles.

Particle agglomeration needs to be considered in two extremes:

1. Regime of particle coalescence where particles are formed into perfect spheres.
2. Regime of agglomeration where fractals are generated with the constants D_f and k_f .

The mean free path decrease with increasing pressure. This results in that coagulation switches to the transition and continuum regimes. Soot particles aggregate into fractal agglomerates. In simulating a non-premixed flame, the integration starts with the coalescent limit and changes to the aggregation limit when the critical diameter d^* is reached. The transformation is done slowly using a $\tanh(\mathcal{D}(d_p))$ in order to avoid convergence problems. $\mathcal{D}(d_p) \propto d_p$ is a function of the particle diameter. Agglomerates are formed through the coagulation process where the particles build fractals. This can be modelled with the method of moments. Again the system has to be divided into three spaces: the free molecular regime, the transition regime and the continuum regime.

Agglomeration formation in the free molecular regime.

The collision frequencies for the free molecular regime f used are [92] given by:

$$\beta_{ij}^{f,a} = 2.2 \sqrt{\frac{\pi k_B T}{2m_1} \left(\frac{1}{m_i} + \frac{1}{m_j} \right)} (d_{c,i} + d_{c,j})^2 \quad (5.29)$$

Similar to coagulation in the Free Molecular Regime, in section 5.2.1, the source terms of the agglomeration for the soot moments may be formulated as

functions of $\langle \Phi_{x,y} \rangle$:

$$\mathfrak{S} M_{r,agg}^f = \frac{1}{2} \sum_{k=1}^{r-1} \binom{r}{k} \langle \Phi_{x,y} \rangle \mathfrak{S} M_0^2 \quad (5.30)$$

with

$$\langle \Phi_{x,y} \rangle = C \langle f_{x,y}^l \rangle \quad (5.31)$$

where $\langle f_{x,y}^l \rangle$ is obtained through the following relation:

$$\begin{aligned} \langle f_{x,y}^l \rangle &= \frac{1}{M_0^2} \sum_{i=1}^{\infty} \sum_{j=1}^{\infty} (m_i + m_j)^l \\ &\cdot (m_i^{1/3} n_i^{1/D_f-1/3} + m_j^{1/3} n_j^{1/D_f-1/3})^2 m_i^{x-1/2} m_j^{y-1/2} N_i N_j \\ &= \sum_{k=0}^l \binom{l}{k} \langle m^{x+k+1/6} n^{2/D_f-2/3} \rangle \mu_{x+k-1/2} \\ &+ 2 \langle m^{x+k-1/6} n^{2/D_f-1/3} \rangle \langle m^{y+l-k-1/6} n^{1/D_f-1/3} \rangle \\ &+ \mu_{(x+k-1/2)} \langle m^{y+l-k+1/6} n^{2/D_f-2/3} \rangle \end{aligned} \quad (5.32)$$

$\langle m^r n^{r'} \rangle$ are binary moments of a two-dimensional particle size distribution, which is a function of the mass of the agglomerate m and the number of primary particles in the agglomerate n . The binary moments are approximated to be functions of the particle mass moments μ_r and the number of primary particles $\pi_{r'}$ [92]

$$\langle m^r n^{r'} \rangle \approx \langle m^r \rangle \langle n^{r'} \rangle = \mu_r \pi_{r'} \quad (5.33)$$

where

$$\pi_r = \frac{P_r}{P_0} \quad (5.34)$$

and

The value of $\langle f_{x,y} \rangle$ is determined by Lagrange interpolation between the logarithms of ${}^0 f_{x,y}, {}^1 f_{x,y}, {}^2 f_{x,y}, \dots, {}^r f_{x,y}$ can even be an expression of the moment formulation [53]

$$\begin{aligned} {}^r f_{x,y} &= \mu_{(k+x+\frac{1}{6})} \mu_{(r+y-k-\frac{1}{2})} + 2\mu_{(k+x-\frac{1}{6})} \mu_{(r+y-k-\frac{1}{6})} \\ &+ \mu_{(k+x-\frac{1}{2})} \mu_{(r+y-k+\frac{1}{6})} \end{aligned} \quad (5.35)$$

The fractional moments $\mu_r = \frac{\mathfrak{S} M_r}{\mathfrak{S} M_0}$. Lagrange interpolation is used to obtain the fractional moments and the expression of ${}^r f_{x,y}$.

Agglomeration in the continuum regime.

The collision frequencies for the free molecular regime f used are [92]:

$$\beta_{ij}^{c,a} = K \left(\frac{C_i}{d'_{c,i}} + \frac{C_j}{d'_{c,j}} \right) (d_{c,i} + d_{c,j})^2 \quad (5.36)$$

The particle diameter $d'_{c,j}$ is the mobility diameter [139]. In order to avoid discontinuity in G_r the suggestion of Kruis et al [140] is followed and the mobility diameter is equated to d_c .

$$\begin{aligned} G_r^f &= \frac{1}{2} K \sum_{k=1}^{r-1} \binom{r}{k} \left[2\mu_k \mu_{r-k} \right. \\ &+ \langle m^{k+1/3} n^{1/D_f-1/3} \rangle \langle m^{r-k-1/3} n^{1/3-1/D_f} \rangle \\ &+ \langle m^{k-1/3} n^{1/3-1/D_f} \rangle \langle m^{r-k+1/3} n^{1/D_f-1/3} \rangle \\ &+ 2.514\lambda \left(\frac{\pi\rho}{6m_1} \right)^{1/3} \left(\langle m^{k-1/3} n^{1/3-1/D_f} \rangle \mu_{r-k} \right. \\ &+ \mu_k \langle m^{r-k-1/3} n^{1/3-1/D_f} \rangle \\ &+ \langle m^{k+1/3} n^{1/D_f-1/3} \rangle \langle m^{r-k-2/3} n^{2/3-2/D_f} \rangle \\ &\left. + \langle m^{k-2/3} n^{2/3-2/D_f} \rangle \langle m^{r-k+1/3} n^{1/D_f-1/3} \rangle \right] M_0^2 \end{aligned} \quad (5.37)$$

Agglomeration in the transition regime.

The transition regime is the intermediate regime between the free molecular and the continuum regime. As for the coagulation into spheres 5.2.1, the semi empirical formula of Fuchs [133] is used to describe the coagulation in the transient regime.

$$\mathbf{s}\dot{G}_{r,agg} = \frac{\mathbf{s}\dot{M}_{r,agg}^f \mathbf{s}\dot{M}_{r,agg}^c}{\mathbf{s}\dot{M}_{r,agg}^f + \mathbf{s}\dot{M}_{r,agg}^c}, \quad r = 0, 2, 3, 4\dots \quad (5.38)$$

Moments for primary particles.

In the regime of coalescence the moments describe the size distribution of the soot particles, which coincide with the primary particles, since they consist of exactly one primary particle. Entering the regime of agglomeration soot particles denominate agglomerates as well as single primary particles in the system. An additional source term for the primary particles in terms of the

statistical moments needs to be introduced:

$$P_r = \sum_{i=1}^{\infty} n_i^r N_i \quad (5.39)$$

where N_i is the concentration of the agglomerate size class i , n_i is the number of primary particles in size class i and $P_0 = M_0$ is the total number density of the soot particles in both regimes. For the regime of coalescence this implies that $n_i = 1$ and the moments of the primary particles P_r coincide with the 0 - th soot moment and thereby:

$$P_r = P_0 = M_0 \quad (5.40)$$

In the agglomeration regime particles consist of more than one primary particle, $n_i > 1$ and P_1 is the total number density of primary particles in the system. They are either free primary particles or joined in an agglomerate. The mean number of primary particles in an agglomerate \bar{n} is given by:

$$\bar{n} = \frac{P_1}{P_0} \quad (5.41)$$

The source term for the Primary Particles in terms of the method of moments reads as:

$$\dot{P}_r = R_0 + H_r, \quad r = 2, 3, \dots \quad (5.42)$$

where R_0 is the rate of particle formation and H_r comes from the aggregate coagulation, with

$$H_r = \frac{1}{2} \sum_{k=1}^{r-1} \binom{r}{k} \left(\sum_{i=1}^{\infty} \sum_{j=1}^{\infty} n_i^k n_j^{r-k} \beta_{ij}^a N_i N_j \right) \quad (5.43)$$

where the collision frequency differs for the different regimes:

Moments for primary particles in the free molecular regime.

In the free molecular regime :

$$H_r^f = \frac{1}{2} \langle \psi_r \rangle \quad (5.44)$$

with

$$\frac{1}{2} \langle \psi_r \rangle = C \cdot \langle h_r \rangle \quad (5.45)$$

where C is given in equation (3.7) and $\langle h_r \rangle$ can be determined with:

$$\begin{aligned} \langle h_r \rangle &= \sum_{k=0}^l \binom{r}{k} \left(\langle m^{k+1/6} n^{q+2/D_f-2/3} \rangle \langle m^{l-k-1/2} n^{r-q} \rangle \right. \\ &+ 2 \langle m^{k-1/6} n^{q+1/D_f-1/3} \rangle \langle m^{l-k-1/6} n^{r-q+1/D_f-1/3} \rangle \\ &+ \left. \langle m^{k-1/2} n^q \rangle \langle m^{l-k-1/6} n^{r-q+2/D_f-2/3} \rangle \right) \end{aligned} \quad (5.46)$$

5.2.3 Agglomeration in the continuum regime.

For the continuum regime we have that:

$$\begin{aligned} H_r^f &= \frac{1}{2} K \sum_{k=1}^{r-1} \binom{r}{k} \left[2\pi_k \pi_{r-k} \right. \\ &+ \langle m^{1/3} n^{k+1/D_f-1/3} \rangle \langle m^{-1/3} n^{r-k+1/3-1/D_f} \rangle \\ &+ \langle m^{-1/3} n^{k+1/3-1/D_f} \rangle \langle m^{1/3} n^{r-k+1/D_f-1/3} \rangle \\ &+ 2.514\lambda \left(\frac{\pi\rho}{6m_1} \right)^{1/3} \left(\langle m^{-1/3} n^{k+1/3-1/D_f} \rangle \pi_{r-k} \right. \\ &+ \pi_k \langle m^{-1/3} n^{r-k+1/3-1/D_f} \rangle \\ &+ \langle m^{1/3} n^{k+1/D_f-1/3} \rangle \langle m^{-2/3} n^{r-k+2/3-2/D_f} \rangle \\ &+ \left. \left. \langle m^{-2/3} n^{k+2/3-2/D_f} \rangle \langle m^{1/3} n^{r-k+1/D_f-1/3} \rangle \right) \right] M_0^2 \end{aligned} \quad (5.47)$$

5.2.4 Moments for primary particles in the transition regime.

For the transition regime the semi empirical formula of Fuchs [133] is used:

$$\mathbf{s}\dot{H}_r = \frac{\mathbf{s}\dot{H}_r^f \mathbf{s}\dot{H}_r^c}{\mathbf{s}\dot{H}_r^f + \mathbf{s}\dot{H}_r^c}, \quad r = 0, 2, 3, 4... \quad (5.48)$$

5.3 Transition between coalescent to fractal regime

The Transition between the formation of primary particles and agglomerates is still not understood very well. The process has been subject of different studies [2, 141]. Many models are based on the idea that particles coalesce until they reach a critical size, at which they do not have sufficient time to fuse

[141, 142]. Other theories suggest that particles grow through a simultaneous surface growth and agglomeration [123].

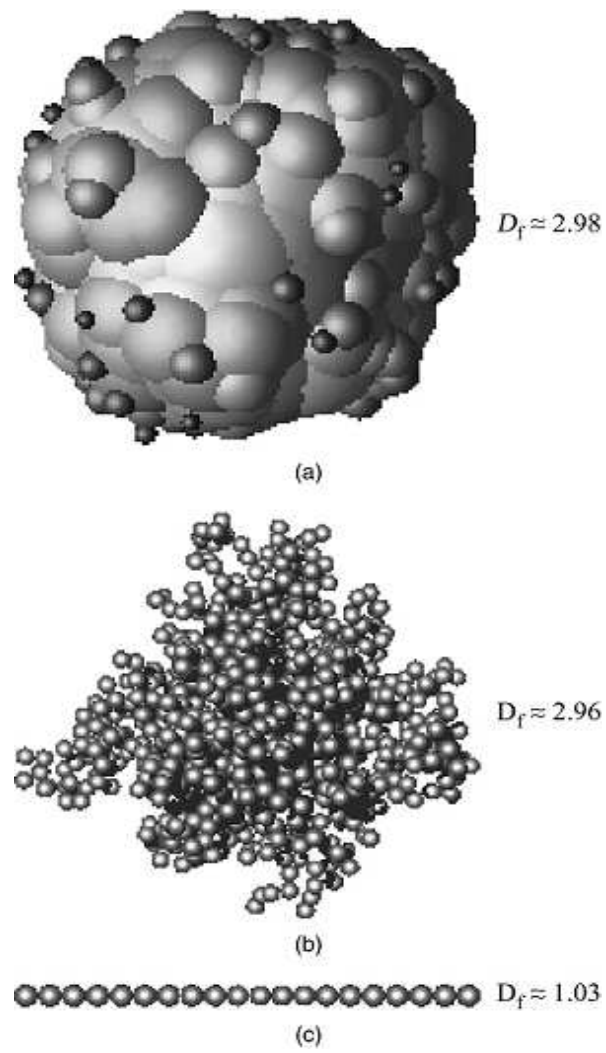


Figure 5.5: Fractal dimension for three aggregates in R^3 : (a) 320 balls, (b) 1 500 balls, (c) 20 balls taken from [141]

Many studies seek to describe the surface behavior of particles. The more granular a particle is the more surface is accessible for reactive species. The fractal diameter introduced in equation 5.28 of the previous subsection is a limited shape descriptor of the agglomerate and (see figure 5.5). The fractal dimension does not link 5.5 (b) and (c) even though they are more alike in their granular structure. The study therefore focusses on describing the trajectory of a particle in a sphere-normalized volume/surface space. The result is the *delta-and Delta* method based on critical parameters (δ, Δ) , defined as:

$$\delta = \frac{d - 2/3}{1 - d} \quad (5.49)$$

$$\Delta \equiv \frac{D - 2/3}{1 - D} \quad (5.50)$$

with

$$D = \frac{d(\ln s)}{d(\ln v)}, d \in [\frac{2}{3}, 1] \quad (5.51)$$

where v is the the sphere-normalized volume

$$v = \frac{V}{V_0} \text{ and } s = \frac{S}{S_0} \quad (5.52)$$

where V is the volume and $V_0 = \frac{4}{3}\pi R_0^3$ and where S is the surface and $S_0 = 4\pi R_0^2$

$$s = v^d \quad (5.53)$$

δ indicates whether the particles is in the coalescent regime ($\delta < 1$) or the fractal regime ($\delta < 1$) while Δ is a measure for the direction of the trajectory. This model was applied in a combustion code by Balthasar and Frenklach [143] to introduce the total surface area of the ensemble of soot particles.

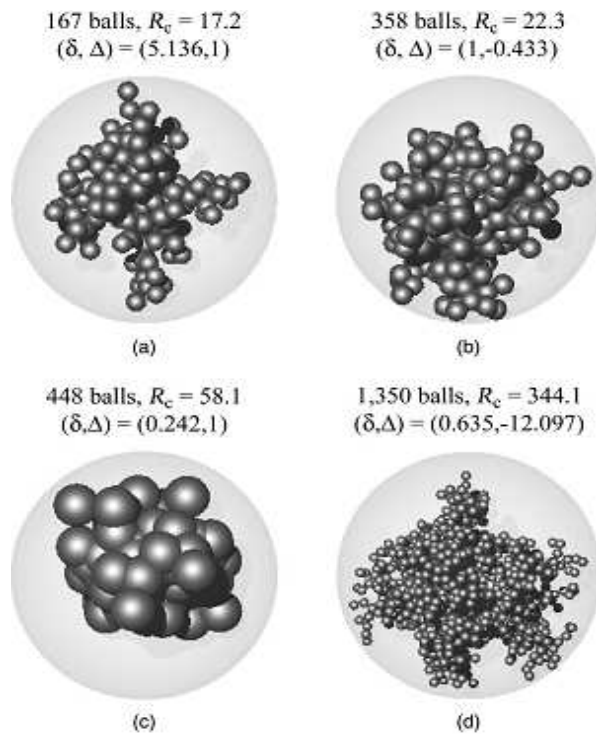


Figure 5.6: Examples for the different agglomerates in different points of the (δ, Δ) -regime taken from [141]

5.4 Sectional model of soot formation

The sectional model is similar to the momentum method. It treats the process of soot formation on the basis of particles size distribution. The method accounts both for physical and chemical processes are accounted for. The method bases on methods by Gelbard et al. [144, 144], which deal with general formation of aerosol formation. The results of Gelbard et al. will be discussed in chapter 7. The approach was first applied on soot formation by Colket et al. [145]. The sectional method is a tool to predict the processes early in the flame, but also the process of surface growth, coagulation and agglomeration. The only constraint is that k should be as large as the lower size of detection limit. Nucleation can be defined as the agglomeration of two monomers of size k and condensation as the net agglomeration rate of a monomer with a cluster. The kinetic of soot formation is modeled (section 2.1.2) up to the growth of spherical solid carbon surface growth in the free molecular limit. The further growth of soot spheroids is then modeled as an aerosol dynamics problem, involving the division of the size class mass densities with terms representing Particle inception, surface growth, oxidation and coagulation. The particles are assumed to contain carbon only. Soot spheroids vary in diameter in an interval from 1 to 100 nanometers and variation of 6 orders of magnitudes in mass. Colket et al. assumed that the boundaries of the sections are log normal distributed. The sectional boundaries will be given by

$$D_\ell = D(0) \left(\frac{D(M)}{D(0)} \right)^{\ell/M} \quad (5.54)$$

where M is the number of sections with diameter minima $D(0)$ and maxima $D(M)$. The particle mass is given by

$$m = \rho_s \frac{\pi D^3}{6} \quad (5.55)$$

and ρ_s is the density of carbon. The mass of the section is then given by:

$$Q_\ell = \int_{m_{\ell-1}}^{m_\ell} m n_\ell(m, t) dm \quad \implies \quad (5.56)$$

$$n_\ell(m, t) = \frac{Q_\ell}{m^2} \Delta_\ell \quad (5.57)$$

where

$$\Delta_\ell = \left(\ell n \frac{m_\ell}{m_{\ell-1}} \right) \quad (5.58)$$

leading to a definition of number density N_ℓ and average mass \bar{m}_ℓ of particles in section ℓ :

$$N_\ell = b \int_{m_{\ell-1}}^{m_\ell} n_\ell(m, t) dm \quad (5.59)$$

$$\begin{aligned} &= Q_\ell \Delta_\ell \left(\frac{1}{m_{\ell-1}} - \frac{1}{m_\ell} \right) \bar{m}_\ell \\ &= \frac{\int_{m_{\ell-1}}^{m_\ell} m n_\ell(m, t) dm}{\int_{m_{\ell-1}}^{m_\ell} n_\ell(m, t) dm} \\ &= \Delta_\ell^{-1} = \left(\frac{1}{m_{\ell-1}} - \frac{1}{m_\ell} \right) \end{aligned} \quad (5.60)$$

The lowest order intra-class density function $\frac{dQ_\ell}{dln(m)}$ is assumed to be constant within a section. The net rate of growth due to surface mass addition and oxidation for a particle is assumed to be proportional to the particle surface area:

$$\frac{dm}{dt} = G'(A) = G(t)m^{2/3}, \quad (5.61)$$

where A is the surface of the particle and $G'(t) = R_{sg} - R_{ox}$. R_{sg} is the rate of surface growth by acetylene and R_{ox} the oxidation of the soot particles. Hence, the dynamic balance equation for Q_{ell} is given by:

$$\begin{aligned} \frac{dQ_\ell}{dt} &= \frac{1}{2} \sum_{i=1}^{\ell-1} \sum_{j=1}^{\ell-1} {}^1\bar{\beta}_{i,j,\ell} Q_i Q_j \\ &- Q_\ell \sum_{i=1}^{\ell-1} {}^2\bar{\beta}_{1,j,\ell} Q_1 - \frac{1}{2} {}^3\bar{\beta}_{\ell,\ell} Q_\ell^2 \\ &- Q_\ell \sum_{i=\ell+1}^M {}^4\bar{\beta}_{i,\ell} Q_i + {}^1G_\ell Q_\ell + {}^2G_{\ell+\ell_N} Q_{\ell+\ell_N} - {}^2G_\ell Q_\ell \delta_{\ell 1} S_i(t) \end{aligned}$$

where:

$$\ell_N = -1 \quad G(t) > 0 \quad \ell_N = 1 \quad G(t) < 0$$

β are the intersectional collisions coefficients and G_ℓ the growth coefficients. S_i is the rate for particle inception, with:

$$\begin{aligned} {}^1\bar{\beta}_{i,j,\ell} &= \Delta_i \Delta_j \int_{X'_{i-1}}^{X'_i} \int_{X_{j-1}}^{X_j} \frac{\bar{\mathbf{H}}\mathbf{H}(m - m_{\ell-1} + m_\ell - m')(m + m')\beta(m, m')}{mm'} dX dX' \\ {}^2\bar{\beta}_{i,\ell} &= \Delta_i \Delta_\ell \int_{X'_{i-1}}^{X'_i} \int_{X_{j-1}}^{X_j} \frac{\bar{\mathbf{H}}(\mathbf{H}(m + m' - m_\ell)m - \mathbf{H}(m_\ell - m - m')m')\beta(m, m')}{mm'} dX dX' \\ {}^3\bar{\beta}_{\ell,\ell} &= \Delta_\ell^2 \int_{X'_{\ell-1}}^{X'_\ell} \int_{X_{\ell-1}}^{X_\ell} \frac{\bar{\mathbf{H}}\mathbf{H}(m + m' - m_\ell)(m + m')\beta(m, m')}{mm'} dX dX' \\ {}^4\bar{\beta}_{i,\ell} &= \Delta_i \Delta_j \int_{X'_{i-1}}^{X'_i} \int_{X_{\ell-1}}^{X_\ell} \frac{\mathbf{H}(m - m_{min})\beta(m, m')}{m'} dX dX', \end{aligned}$$

where $\mathbf{H} = \int_{-\infty}^x \delta(y) dy$ is the Heaviside function and $\bar{\mathbf{H}} = \mathbf{H}(m - m_{min})\mathbf{H}(m' - m_{min})$. The soot volume fraction is then given by

$$f_v = \frac{1}{\rho_s} \sum_{ell} Q_\ell \quad (5.62)$$

The previous studies apply statistical methods in order to predict further growth and even growth of particles. This can also be done in terms of chemical methods. Studies can be retrieved in literature, that define reaction rates larger carbonaceous structures such as fullerene, c_{60} [146]

5.5 Atmospheric aging processes

Aging of aerosols has even been subject of large uncontrolled forest fire of the size $3.9 \cdot 10^4$ ha of timber that burned for over one month in 1987 in Grant's Pass, Oregon, USA. The dispersion of the smoke plume was exceptionally slow due to special weather conditions. The low dispersion rate allowed a high particle concentration over the period of the measurements which were performed by Radke et al. [147]. Particles at the center of plume were collected using a Convair C-131A research aircraft. The samples were taken at three timesteps: 10, 25 and 44 h. Figure 5.7 shows one result of the analysis where we see a further decrease of number density and an increase in diameter.

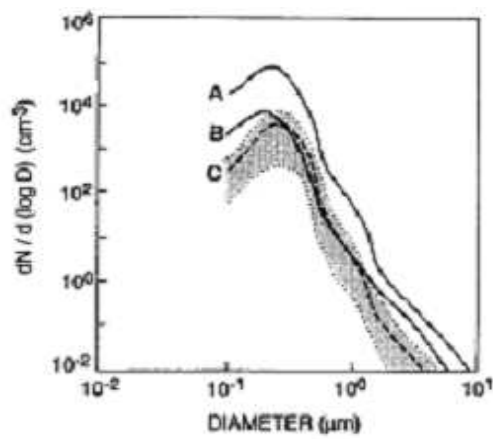


Figure 5.7: Examples for the different agglomerates in different points of the (δ, Δ) -regime taken from [147]

Chapter 6

Heterogeneous reactions

The study of aerosol formation is often limited to homogeneous particles. However, multi-component aerosol particles have a high industrial importance- [148] and there is a need for significant research activity in this domain. Heterogeneous reactions of the reactive soot particles with a number of gas phase species is therefore of interest. The reactivity of soot or black carbon has been topic of few studies. Applying Fourier transform infrared (FT-IR) spectroscopy Smith and Chughtai found in 1995 the soot structure well suited for heterogeneous reactions with oxidant molecules at temperatures up to 700 °C [149]. The reactivity of carbon and soot has been known since long. Carbon industries have designed *activated carbons* to remove impurities and act as reducing agents [90]. In industrial carbon production soot is rapidly cooled in order to maximize the reactive surface area of the particles. Table 6.1.3, taken from Mulholland et al. [90], lists sublethal effects of different species and their potential sources.

6.1 Classes of heterogeneous reactions

The group of reactions of soot particles with gas phase species can be organized into three different classes. This discussion follows Mulholland et al. [90].

6.1.1 Polar and paramagnetic molecules

The following species are polar molecules and carry a molecular dipole moment: $HCHO$, HF , HCl , HBr , CO , NH_3 , NO and H_2O . Those species are most likely adsorbed by the radical sites (see section 5.1). The adsorption of water molecules onto the surface enhances the adsorption of other polar

molecules. This process is relevant in fires, where large amounts of water vapor are released. Paramagnetic molecules, such as O_2 , NO_2 , and NO have unpaired electrons with parallel spins. They are highly adsorbent by any charged matter. Since soot contains many sites carrying unpaired electrons, the attraction of paramagnetic molecules is strong.

6.1.2 Aromatic molecules

Heterogeneous reactions with aromatics are previously described in chapter 5. Many studies can be found describing these processes.

6.1.3 Transport of toxic gases by soot particles

Butler et al. [90] lists a number of toxic species which are soot adsorbents. On one hand the concentration in the gas phase transport plays a more significant role than the raised concentration due to heterogeneous reactions with particles. On the other hand critical concentrations are often only measured considering the gas phase, while the additional concentrations on the soot is ignored. At the same time the lethal dose of those species is low and the particles enable a long range transport of the adsorbents.

6.2 Heterogeneous reactions in the flame

Heterogeneous reactions with soot particles have had very limited attention from the combustion society regarding reactions within the flame. The processes considered in literature have been mentioned in the previous chapters. One is the adsorption of acetylene in the process of surface growth, the other is the reaction with oxygen in hotter domains of the flame.

6.3 Heterogeneous reactions in the post flame

Surface adsorption of HCl has been the toxicity of hydrogen chloride, HCl , released from the decomposition of poly vinyl chloride in fires, has received considerable attention. Studies on toxic adsorbents other than the above mentioned have been performed by Hertzberg et al. [20]. The study presents an identification of isocyanates on particles from combustion of different materials, relevant in fires. The analysis is done under application of FT-IR spectroscopy, and LC-MS technique. The study even described the distribution of the particles diameter determined using a DEKATI low pressure impactor [150]. Galoway et al. demonstrated that significant amounts of HCl readily adsorb on

and then react with and/or diffuse into many types of common interior surfaces. Even though the model was further developed and introduced into FAST [151]. Little or no detailed modeling of heterogeneous reactions explaining the process has yet been performed.

6.4 Heterogeneous reactions in atmosphere

A more extended list of literature exists describing the heterogenous processes in outer atmosphere. A large series of experimental studies revealing heterogeneous reactions between soot particles and different gas phase species in conditions relevant in the outer atmosphere have been performed by Smith and Chughtai et al. [149, 152, 153, 154]. The work documents reactions with gas phase species such as SO_2 , O_3 , NH_3 , NO_2 , NO and the corresponding reaction rates. They even found reactions with H_2O [152], which is topic of chapter 7. The adsorption of other gases of particular concern in fires i. eg. acrolein have not been studied.

6.5 Reduction of the formation of soot by heterogeneous reactions with additives.

Heterogenous reactions of soot particles with species from the gas phase may also imply a reduction of growth of soot particles. Controlling and reducing the formation of soot in different combustion processes and with different fuels are topic of a number of studies [155, 156, 157].

About 40 additives have been tested for their ability to reduce soot formation in a premixed propane-air flame [158]. Furthermore experiments on the suppression of soot formation through additives showed that the processes are depend on the combustion devices.

Experiments on the effect of additives such as Lubrizol 565 (a barium containing compound), Ferrocene [159], MMT (magnesium containing compounds) [160] and additives containing magnesium, barium and calcium [161] have been tested in kerosene combustion gas turbine devices. In this devices the Lubrizol gave a significant reduction in soot, but left deposits at the chamber walls. Ferrocene did not result in any reduction, MMT also reduced soot emission and the performance.

The additives have also tested in diesel engines. Ray and Long [162] tested a number of nonmetallic additives such as nitroethane, 1-nitropropane, ethyl nitrate and t-butylhydroperoxide (t-BuOOH) and found the latter to be most effective. An addition of 5% t-BuOOH resulted in a 30% reduction of particles

and a 50% of benzo[a]pyrene. Lubrizol resulted in a reduction of particles up to 50% and the addition of 0.075% Barium led to an decrease of up to 20% [157].

Studies on additives in domestic boilers combusting oil have been performed with following additives:

- Ferrocene was most effective followed in order by nickel, cobalt, magnesium [163].
- Vaerman [164] achieved an 80% reduction by weight in flue-gas soot using different metal naphthenates.
- Kukin [165] also achieved an 80% weight reduction of the particulates applying Magnesium oxide in the furnace.

Some of the above mentioned reactions affect the reactions in the gas phase only, others such as Mn, Fe, Co and Ni affect the process of soot formation by lowering the oxidation to $120^{\circ}C$ as the case for Mn and Ferrocene. Cotton, Friswell and Jenkins made the adsorption of the metals onto the soot particles responsible for the reduction in soot growth [158].

Table 6.1: Sublethal effects occurring: A, below 10^{-5} volume fraction (10 ppm by volume); B, 10^{-5} to 10^{-4} volume fraction (tens of ppm by volume); C, at 10^{-4} to 10^{-3} volume fraction (hundreds of ppm by volume); D, at 10^{-3} to 10^{-2} volume fraction (thousands of ppm by volume. Table is taken from Mullholland et al. [90].

Toxic gas	Potential sources	Sublethal effects
Acrolein ($CH_2 = CHCHO$)	Cellulosic materials, e.g., wood, cotton, paper, polystyrenes, ABS	A
Toluene diisocyanate (TDI)	Flexible polyurethane foams	A
Formaldehyde ($HCHO$)	POM, polypropylenes	B
Hydrogen cyanide (HCN)	Nitrogen-containing materials, e.g. wool, silk, PAN, ABS, acrylic fibers, nylons, urea/formaldehyde, melamine, polyurethanes, polyacrylamide	C
Nitrogen dioxide (NO_2)	Nitrogen-containing materials	B
Hydrogen chloride (HCl)	PVC and chlorinated additives	B, D
Hydrogen fluoride (HF)	PTFE, other fluorinated compounds and additives	B
Hydrogen bromide (HBr)	Brominated compounds and additives	B, D
Sulfur dioxide (SO_2)	Sulfur-containing materials, e.g. wool, vulcanized rubbers, poly(phenylene sulfide)	B
Hydrogen sulfide (H_2S)	Sulfur-containing materials	C
Ammonia (NH_3)	Nitrogen-containing materials	C
Styrene (C_8H_8)	Polystyrenes, ABS	C
Toluene (C_7H_8)	Polystyrenes, PVC, polyurethane foams	D
Benzene (C_6H_6)	Polystyrenes, PVC, polyesters, nylons	C

Chapter 7

Droplets

The formation of droplets has many similarities to the formation of solid particles. In addition depends on the formation of solid particles since the heterogeneous reaction of a soot particle with the polar water molecule, H_2O , is the most frequent nucleation process (see section 6.1). The process of droplet formation and evaporation consists of a number of steps, with similarities to the formation of solid particles such as soot. The steps are described below and graphically presented in figure 7.1.

The four above listed steps in droplet formation and reduction depend on the saturation ratio R_{Sat} of the domain:

$$R_{Sat} = \frac{p}{p_s} \quad (7.1)$$

The saturation ratio is a function of the equilibrium vapor pressure for a plane liquid surface p_s , a partial pressure, and the pressure p . For water in mm Hg and temperatures in $T \in [0 - 60]^\circ C$ p_s can be defined as [166]:

$$\log_{10} p_s = 8.11 - \frac{1750}{T + 235} \quad (7.2)$$

Three different states of droplets, related to the saturation ratio can be identified. The states depend on droplet size and humidity. There are:

1. Unsaturated vapor, $R_{Sat} < 1$: Nucleation leads to the formation of unstable droplets, which tend to disintegrate into smaller droplets.
2. Saturated vapor, $R_{Sat} \sim 1$: This is the most stable state of droplets. Nucleation and coagulation lead to the formation of stable droplets. Collision of droplets leads to coagulation or disintegration. This process also depends on the collision velocity and the viscosity of the fluid.

3. Supersaturated vapor, $R_{Sat} > 1$: Nucleation, coagulation and collision lead to droplet disintegration.

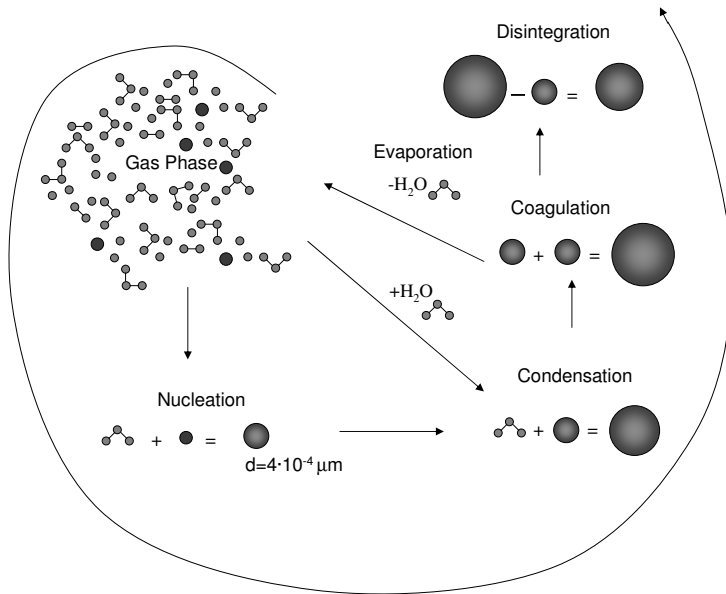


Figure 7.1: Formation and evaporation of droplets.

Kelvin effect

As stated above, saturation vapor pressure is defined as the equilibrium partial pressure for a plane surface at a given temperature. The pressure depends on the shape of the object. The partial pressure required to maintain equilibrium increases with the curvature. The smaller the droplet the easier it is for molecules to leave the droplet surface. Little evaporation implies that the mass equilibrium is kept. Hence, the partial pressure of vapor must be greater than p_s . The saturation ratio is related to the critical diameter at which the droplet is stable [166]:

$$\frac{p}{p_s} = \exp \left[\frac{4\gamma M}{\rho RT d^*} \right] \quad (7.3)$$

where γ is the surface tension, M the molecular weight and ρ the density of the liquid. d^* is the Kelvin diameter, the critical diameter for a stable droplet. If the droplet diameter exceeds d^* , the droplet grows and for diameters smaller than d^* , it evaporates.

7.1 Six steps of droplet formation

The description of droplet formation, described in follows figure 7.1.

7.1.1 Gas - and solid phase

The first reactions leading to nucleations, occur in the gas phase. The gas phase is assumed to contain all kinds of single molecular species, but also particles such as soot particles. Species from the gas and the solid phase are the building stones for the formation of liquid and solid aerosols. Those particles are formed through homogeneous and heterogeneous reactions.

7.1.2 Homogeneous nucleation

Homogeneous nucleation is the formation of particles from a supersaturated vapor ($R_{sat} > 1$) without the assistance of condensation nuclei or ions. This process is also called self-nucleation. It is a rare phenomenon which mostly is laboratory generated. Here attractive forces between the molecules lead to the formation of droplets. This can even happen in unsaturated vapor. Unstable droplets are formed in this process and tend to disintegrate. The rate of particle growth through homogeneous nucleation is given by:

$$\frac{d}{dt} d_p = \frac{2M(p - p_d)}{\rho_p N_a \sqrt{2\pi m k T}} \quad \text{for } d_p < \lambda \quad (7.4)$$

$$\frac{d}{dt}d_p = \frac{4D_v M(p - p_s)}{RT\rho_p d_p} \quad \text{for } d_p > \lambda \quad (7.5)$$

λ is the gas mean free path, M is the molecular weight, m the mass of the vapor molecule, D_v the diffusion coefficient of the vapor molecule, and p_d the partial pressure of the curved droplet surface.

7.1.3 Heterogeneous nucleation

Nucleated condensation or heterogeneous nucleation is the process where condensation nuclei or ions such as soot particles react with species from the gas phase such as H_2O and build larger molecular clusters, as previously described in section 6.1.1. This is the most common phenomenon responsible for the formation of droplets. Whereas homogeneous nucleation usually requires saturation ratios of 2-10, nucleated condensation can occur at undersaturate states.

The hydration of soot particles is topic of a number of studies [167, 168, 90]. Chughtai et al. [167] found an amplifying effect of the adsorption of water molecules. The adsorptiveness of H_2O molecules increases with the number of adsorbed H_2O molecules.

7.1.4 Condensation and coagulation

The process of condensation is also a heterogeneous process. It begins when enough water has been adsorbed onto the soot surface and a droplet has been formed. Condensation is the heterogeneous reaction where H_2O molecules are adsorbed by the liquid aerosol.

7.1.5 Coagulation

Analogous to the process of formation of soot particles, droplets coagulate and built larger droplets. Experiments and dynamics of droplet collisions have been studied by Willis and Orme [169].

7.1.6 Evaporation

Evaporation is the abstraction of H_2O molecules into the gas phase. Evaporation is the reverse of growth by condensation. In this process more molecules leave the particle surface than arrive. With evaporation there is no counterpart to the threshold of formation that must be reached for condensation to commence, and droplets of pure liquid will evaporate completely. The evaporation

rate is defined analogous to equation 7.4 and 7.5:

$$\frac{d}{dt}d_p = \frac{4D_v M}{R\rho_p d_p} \left(\frac{p_\infty}{T_\infty} - \frac{p_d}{T_d} \right) \quad \text{for } d_p > \lambda \quad (7.6)$$

leading to the definition of the evaporation time:

$$t = \frac{R\rho_p d_p^2}{8D_v M \left(\frac{p_d}{T_d} - \frac{p_\infty}{T_\infty} \right)} \quad (7.7)$$

The *Fuchs effect* 5.2.1 is based on the assumption that transport of vapor molecules from the surface of a droplet to an imaginary concentric sphere of diameter $d_p + \frac{4}{3}\lambda$ is controlled by the kinetic theory of gases. Beyond this imaginary sphere the rate of evaporation is governed by diffusion and follows equation 7.7

7.1.7 Disintegration

Disintegration is one process of size reduction of droplets. Here one droplets disintegrates into two droplets of smaller size.

7.1.8 Modeling the formation of droplets

This subsection will shortly discuss methods applicable for modeling the formation of droplets. The models follow are in priciple the same as for soot fromation and have been subject of previous chapters.

A number of articles can be found applying the Smoluchowski equation [170], the method of moments 2.1.2 [171, 172], but also the sectional method, section 5.4. The approach covers two methods: the discrete and the continuous method, which both can be retrieved in Gelbard et al. [144]. The models have in common that the aerosol is divided into sections, and an equation is written for each section including the regimes: coagulation, surface growth and oxidation. For the smallest section, an inception source term is included. A general chemical inception model [173] and radiative loss can be included. The sectional method could be defined as a more promising approach in terms of CPU time than the method of moments. The method bases on a population balance equation where the volume v is a conserved variable. Gelbard et al. suggested to part the total of the infinite number of size classes into two, separated by a critical volume v_k :

- For droplets with volumes $v \leq v_k$ the discrete representation is used.

Hence, the nucleation in this domain is given by:

$$N(\dot{v}_i, t)_{disc} = N_i(v_i, t) \sum_{j=1}^k \beta(v_i, v_j) N(v_j) \quad (7.8)$$

- For droplets with volumes $v > v_k$ the continuous representation is used. The nucleation in the continuous domain is given by:

$$N(\dot{v}_i, t)_{cont} = N_i(v_i, t) \int_{v_{k+1}-v_1/2}^{\infty} \beta(v_i, v) n(v, t) dv \quad (7.9)$$

The total rate of formation is then given in terms of disintegration/evaporation E , the homogeneous surface reactions S_0 and S_1 :

$$\begin{aligned} \dot{N}(v_i, t) &= \frac{1}{2} \sum_{j=1}^{i-1} \beta(v_i, v_j) N(v_{i-j}, t) N(v_j, t) \\ &- N_i(v_i, t) \left[\sum_{j=1}^k \beta(v_i, v_j) N(v_j) \right. \\ &\left. + \int_{v_{k+1}-v_1/2}^{\infty} \beta(v_i, v) n(v, t) dv \right] + \Gamma_i \end{aligned} \quad (7.10)$$

where

$$\Gamma_i = E(v_i) N(v_{i+1}, t) \quad \text{for } 2 \leq i \leq k-1 \quad (7.11)$$

$$\Gamma_i = \int_{v_{k+1}-v_1/2}^{v_{k+1}+v_1/2} E(v_i) N(v_{i+1}, t) \quad \text{for } i = k \quad (7.12)$$

There are two modeling aspects which link the processes for soot formation to the formation of droplets. The formation of droplets can be considered as heterogenous reactions onto particles, where soot is a appropriate candidate. The models used in order to describe the formation and reduction of soot particles are applicable for the formation of droplets. Both soot and droplets are emitted in combustion processes or are built later in atmosphere as a consequence of combustion.

Chapter 8

Conclusion and opened questions

This report gives an overview of achievements in the field of aerosol-formation. The focus is especially on soot and droplets, in and after fires. Opened questions are brought up and will be discussed in this final chapter. Unsolved problems in all areas are identified in the report.

Aerosols are a threat to health, environment and their emission cause expensive damage on material. They present an instantaneous problem in fires since they reduce the visibility and thereby complicate evacuation from fires as well as they present a long term health threat for firemen and -women, which frequently are in contact with these emissions. Their presence in fires affects the flame spread. At the same time the research on the formation of aerosols from fires are fragmental and limited.

Emissions from fires and other combustion processes can not be predicted with the modeling tools available today. Legislation and the work of fire engineers rely on limited, empirical studies [174, 175, 176] and the individual experience. Existing programming tools offer very little chemical modeling, which is needed to predict the formation of aerosols. The goal of future projects should be the inclusion of combustion models accounting for materials involved in fires into CFD models. Achievements of other fields such as the combustion of biomass and waste are useful in this context. It would be beneficial for both fields if synergetic projects were realized.

8.1 Fuels

Extensive studies on fuels involved in fires and the development of reaction mechanisms are needed. The fuel composition determines the paths of particle formation (see chapter 3). More research in this field will enhance the insight in aerosol formation and -composition. The fuel also affects the adsorption of toxic species onto particles as well as the flame spread and the visibility reduction in the cause of fires. Knowing the composition of materials involved in fires as well as the composition of the aerosols is essential for the development of new fire detectors.

The first step is gaining a detailed knowledge on the chemical composition of gaseous fuel involved. The achievements in the field of detailed chemical reaction modeling for simple fuels can be an aid in this work on complex fuels. The combustion chemistry should be included in in CFD codes. Nowadays knowledge in the following three domains is fragmental.

8.1.1 Pyrolysis of fuels

The solid, viscous and gaseous materials which are relevant in fires need to be identified. Thereafter models and experiments should be developed, describing the thermal and chemical processes in the material, leading to the pyrolyzation.

8.1.2 Identification of gas composition

The gas composition from the pyrolyzation of the different fuels need to be identified. This composition varies for the different materials. It also depends on the temperature. Further experiments are needed in this domain. Models describing the heating and the pyrolyzation for the different materials are important.

8.1.3 Detailed reaction schemes

Extensive reaction mechanisms for high temperature reactions of simple fuels are available in literature. These achievements should be extended to complex fuels. As soon as the work gets to expensive in CPU time, the process can be accelerated by a direct implementation of the programs into FPGA chips [71]. The development of detailed reaction schemes for complex fuels should be pushed ahead. However, this is a long term goal. No detailed mechanisms for complex fuels exist today. Therefore experimental research leading to empirical models should step in for now and be have some priority.

8.2 Soot

The effect of soot particles has been discussed thoroughly. The soot formation from simple well know fuels can be described in seven steps. Most detailed methods for modeling the process are methods statistical reduction; the method of moments (section 5.2) and the sectional method (section 5.4) are previously described. The approaches need to be extended for fire relevant fuels.

8.2.1 Aging

Since the process of aging is not well defined, it is associated with different time scales, temperatures and particle sizes. However the author seeks to satisfy all reference systems, since they are linked and relevant to fire modeling. The analysis in the report covers three processes growth: surface growth, coagulation and agglomeration. Most research has been done on premixed flames. Premixed flames are not representative for fires. More research on turbulent diffusion flames is needed. There is much work left to do in all domains. Existing soot models and models for the formation of particles need to be extended in order to be able to describe the process in the combustion of complex fuels. As mentioned in section 3, other paths for the formation of particles need to be considered. A better understanding of aging processes is beneficial for the prediction of flamespread and reduction of visibility in the cause of fires. Thereby it would lead to an improvement of CFD programming tools applied in the field of fire safety engineering. It is also important for the toxicity estimation in fires.

8.2.2 Heterogeneous reactions

Heterogeneous reactions are a very interesting topic. It is an important mechanism of growth and the adsorption of toxic species needs further experiential and numerical investigation. The subject is also interesting since additives also can help to stop the growth of soot particles and is thereby linked to the processes of aging. One has to keep in mind though that some additives may be more polluting than the soot particles themselves. However, adsorbates need to be classified after the relevance for the process of growth, toxicity on long and short timescales as well as for the reduction of soot formation. Reaction rates and -schemes for nanoparticle growth through heterogeneous reactions need to be developed. There are a series of experimental tools capable for identifying adsorbents, ranging from the electron microscope [1, 82, 177] to GC-MS measurements [178].

8.3 Droplets

In a modelers point of view, the formation of droplets has many similarities with the formation of soot particles, even though the processes differ in details as composition and timescales a.o. The report summarizes models applied on water. The existing models can be extended to describe the formation and reduction of aerosols in heterogeneous processes. Research on droplet formation in fires is important since the adsorption of H_2O molecules onto the surface enhances the adsorption of other polar gases. Furthermore, significant water vapor is generated in fire; this process is highly relevant and not very well studied. As mentioned earlier, models on particles can and should be modified to additionally comprehend droplet formation.

8.4 The complete fire model

All research completed in the field of fire modeling should aim at contributing to a total model starting out with the physics and chemistry in the combusted material to the chemistry of the combustion process. The final goal should be to unify this competence with CFD modeling and generate a prediction tool for fires. With nowadays approaches this will lead to high CPU time. Instead of applying the traditional tools for the reduction of chemical mechanisms and data compression, which always imply a loss of information, the process should be accelerated by a direct implementation of the programs into FPGA chips [71].

Bibliography

- [1] Lin, W.; Dam-Johansen, K.; Frandsen, F., “Agglomeration in bio-fuel fired fluidized bed combustors,” *Chemical Engineering Journal*, vol. 96, pp. 171–185, 2003.
- [2] Dederichs, A.S., *Flamelet Modelling of Soot Formation in Diffusion Flames*, Ph.D. thesis, Brandtchnik, LTH, 2004.
- [3] Nilsson, P., *A level-set flamelet library model for premixed turbulent combustion*, Ph.D. thesis, Lund University, 2001.
- [4] Hertzberg, T.; Hahne, A.; Josefsson, C.; Holmstedt, G.; Husted, B., “Vattendimma: Teori, fysik, simulering,” Tech. Rep., Brandforsk, 2003, Brandforsk projekt.
- [5] Hollmann, C.; Gutheil, E., “Flamelet-modeling of turbulent spray diffusion flames based on a laminar spray flame library,” *Combustion Science and Technology*, vol. 135, pp. 175–192, 1998.
- [6] Pruser, D., *Toxicity Assessment of Combustion Products*, The SFPE Handbook of Fire Protection Engineering, 3 edition, 2002.
- [7] Eksborg, A.-L.; Sigfridsson, S.-E.; Mansfeld, J.; Elinder, H.; Widlundh, P., “Brand på herkulesgatan i göteborg, o län, den 29-30 oktober 1998,” Tech. Rep., Statens Haverikommission, 2001, Rapport RO 2001:02 O-07/98.
- [8] Totting, B.; Erlandsson, U., “Dödsbränder 1999,” Tech. Rep., Räddningsverket, 2000.
- [9] Persson, B.; Simonson, M.; Mansson, M., “Utsläp från bränder till atmosfären,” Tech. Rep., SP, Sweden, 1995, SP Report 1995:70.

- [10] Smith, L. E.; Denissenko, M.F.; Bennett, W.P.; Li, H.; Amin, S.; Tang, M.; Pfeifer, G.P. , "Targeting of lung cancer mutational hotspots by polycyclic aromatic hydrocarbons," *Journal of the National Cancer Institute*, vol. 92, pp. 803–811, 2003.
- [11] Birgersson, B.;Sterner, O.;Zimerson, E., *Kemiska hälsorisker, toxikologi i kemisk perspektiv*, Liber Hermods, 1 edition, 1983, ISBN 91-23-92593-0.
- [12] Buringh, E.; Opperhuizen, A., "On health risks of ambient pm in the netherlands," Tech. Rep., Netherlands Aerosol Program, 2002, RIVM report 650010 032.
- [13] Ramesh, A.; Walker, S.A.; Hood, D.B.; Guilln, M.D.; Schneider,K.; Weyand, E.H., "Bioavailability and risk assessment of orally ingested polycyclic aromatic hydrocarbons," *International Journal of toxicology*, vol. 23, pp. 301–333, 2004.
- [14] Nadziejko, C.; Fang K.; Chen, L.C.; Cohen, B.; Karparkin, M.; Nadas, A., "Effect of concentrated ambient particulate matter on blood coagulation parameters in rats," Tech. Rep., Health Effects Insitute, Boston MA, USA, 2002, Research Report No.111.
- [15] Boffetta,P.; Jourenkova, N.; Gustavsson, P., "Cancer risk from occupational and environmental exposure to polycyclic aromatic hydrocarbons," 1997.
- [16] Gustavsson, P.; Evanoff, B.; Hogstedt, C. , "kad risk fr cancer och hjrt-sjukdom bland svenska skorstensfejare 1951 - 1990," in *Svenska Lkaresllskapetets Handlingar 1993*, 1993, vol. 102, p. 3.
- [17] Tonnejck, A.E.G.; ten Berge, W.F.; Jansen, B.P., "Monitoring the effects of atmospheric ethylene near polyethylene manufacturing planrs with two sensitive plant species," *Environmental pollution*, vol. 123, pp. 275–279, 2002.
- [18] Shailaja, M.S.; D'Silva, C., "Evaluation of impact of pah on a tropical fish, oreochromis mossambicus using multiple biomarkers," *Chemosphere*, vol. 53, pp. 835–841, 2003.
- [19] Jacobson, M. Z., "Control of fossil-fuel particulate black carbon and organic matter, possibly the most effective method of slow global warming," *Journal of Geophysical Research*, vol. 107, pp. 4410, 2002.

- [20] Hertzberg, T.; Blomqvist P.; Dalene, M.; Skarping, G., "Particles and isocyanates from fires," Tech. Rep., Brandforsk, 2003, Brandforsk projekt.
- [21] Jin, T., *Visibility and Human Behaviour in Fire Smoke*, The SFPE Handbok of Fire Protection Engineering, 3 edition, 2002.
- [22] Zenghua, Y.; Holmstedt, G., "Cfd and experimental studies of room fire growth on wall lining materials," *Fire Safety Journal*, vol. 27, pp. 201–238, 1996.
- [23] Zenghua, Y.; Holmstedt, G., "Fast, narrow-band computer model for radiation calculations," *Numerical Heat Transfer B*, vol. 31, pp. 61–71, 1997.
- [24] Dahlen, S., "90 insatser varje dygn - i onödan," *Sirenen*, vol. 2, pp. 5–10, 2004.
- [25] Pucci, W.E., "Modeling spot-type smoke detector response, currently available methods and their merits for everyday use," *Fire Protection Engineering*, vol. 7, pp. 36–42, 2000.
- [26] Hjorth, B., "Automatisk brandlarm - onödiga larm," Tech. Rep., Rddningsverket, 2000.
- [27] Persson, B.; Tuovinen, H. , "Cfd simulations with reference to smoke detector response," Tech. Rep., Brandforsk, 1995, Report 622-921, 1995:46.
- [28] Andersson, P.; Blomqvist, J. , "Smoke detection in buildings with high ceilings," Tech. Rep., Brandforsk, 2003, Report 628-011.
- [29] Schifiliti, R.P.; Meacham, B.J.; Custer, R.L.P., *Design of Detection Systems*, The SFPE Handbok of Fire Protection Engineering, 3 edition, 2002.
- [30] Schifiliti, R.P., "Fire detection modeling - the research - application gap," in *In Proceedings of the 12th conference on Automatic Fire Detection*. The Combustion Institute, Pittsburgh, 2001, pp. 1–10.
- [31] Skarander, F., "Brandlamrssystemet ebl512- undersökning a nya algoritmer till tredje generationens sensorer," Tech. Rep., Brandforsk, 1999, Report 5052.
- [32] Worrell, C.L.; Roby, R.J.; Streit, L.; Torero, J.L., "Enhanced deposition, acoustic agglomeration, and chladni figures in smoke detectors," *Fire Technology*, vol. 37, pp. 343–362, 2001.

- [33] Gottuk, D.T.; Peatross, M.J.; Roby, R.J.; Beyler, C.L., "Advanced fire detection using multi signature alarm algorithms," *Fire Safety Journal*, vol. 31, pp. 381–394, 2002.
- [34] Bryan, J.L. , *Behavioural Response to Fire and Smoke*, The SFPE Handbok of Fire Protection Engineering, 3 edition, 2002.
- [35] Maricq, M.M., "Size and charge of soot particles in rich premixed ethylene flames," *Combustion and Flame*, vol. 137, pp. 340–350, 2004.
- [36] Frantzich, H., "Utrymning genom rök i komplexa miljöer som tunnlår: Utrymning genom irriterande och tät rök," Tech. Rep., Brandforsk, 2003, Report 208-021.
- [37] Mulholland, G.W., *Smoke Production and Propperties*, The SFPE Handbok of Fire Protection Engineering, 3 edition, 2002.
- [38] Isaksson, S., "Påverkan av rök på elektronik," Tech. Rep., Sveriges Provnings- och Forskningsinstitut, 2000, Brandforsk projekt.
- [39] Ingason, H., "Brand- och rökspridning i stora industri- och produktion-slokaler," Tech. Rep., Brandforsk, 2004, Report 630-021.
- [40] Nichols, E. L., "On the temperature of the acetylene flame," *Physical Review (Series I)*, vol. 10, pp. 234252, 1900.
- [41] Ravet, F.; Baudoin, C.; Schultz, J.-L., "Modéisation numerique des koulements reactifs dans les foyers de turbor6acteurs," *Revue Générale de Thermique*, vol. 36, pp. 5–16, 1997.
- [42] Huang, X., *Development of Reduced-Order Flame Models for Prediction of Combustion Instability*, Ph.D. thesis, Virginia Polytechnic Institute and State University, 2001.
- [43] Baulch, D.L.; Cobos, C.J.; Cox, R.A.; Esser, C.; Frank, P.; Just, Th.; Kerr, J.A.; Pilling, M.J.; Troe, J.; Walker, R.W.; Warnatz, J., "Evaluated kinetic data for combustion modelling," *Journal of Physical and Chemical Reference Data*, vol. 21, pp. 411–734, 1992, No.3.
- [44] Warnatz, J.; Maas, U.; Dibble, R. W., *Verbrennung*, Springer Verlag, 2 edition, 1996.
- [45] Frenklach, M., "Reduction of chemical reaction models," *Chem. Ing. Sc.*, vol. 40, pp. 1842, 1985.

- [46] Bittner, J.D.; Howard, J.B., "Composition profiles and reaction mechanisms in a near sooting premixed benzene/oxygen/argon flame," in *Eighteenth Symposium (International) on Combustion*. The Combustion Institute, Pittsburgh, 1980, p. 1105.
- [47] Miller, J.H., "The kinetics of polynuclear aromatic hydrocarbon agglomeration in flames," in *Twenty-Third Symposium (International) on Combustion*. The Combustion Institute, Pittsburgh, 1990, p. 91.
- [48] Miller, J.H.; Smyth, K.C.; Mallard, W.G., "Calculations of the dimerization of aromatic hydrocarbons: Implications for soot formation," in *Twentieth Symposium (International) on Combustion*. The Combustion Institute, Pittsburgh, 1984, p. 1139.
- [49] Harris, S.J.; Weiner, A.M., "A picture of soot particle inception," in *Twenty-Second Symposium (International) on Combustion*. The Combustion Institute, Pittsburgh, 1988, pp. 333–342.
- [50] Slagle, I.R.; Park, J.Y.; Heaven, M.C.; Gutman, D.J., "Kinetics of polyatomic free radicals produced by laser photolysis. 3. reaction of vinyl radicals with molecular oxygen," *Journal of the American Chemical Society*, vol. 106, pp. 4356–4361, 1984.
- [51] Westmoreland, P.R., "Thermochemistry and kinetics of $c_2h_4 + o_2$ reactions," *Combustion Science and Technology*, vol. 82, pp. 151, 1992.
- [52] Chiang, H.M.; Lay, T.H.; Bozelli, J.W., "Kinetic modeling: High pressure propane oxidation: Comparison with experiment," in *Fall Technical Meeting of the Eastern States Section of the Combustion Institute, Worcester*, 1995.
- [53] Balthasar, M., *Detailed soot modelling in turbulent diffusion flames*, Ph.D. thesis, Lund University, 2000.
- [54] Blurock, E.S., "Reaction: System for modeling chemical reactions," *Journal of chemical information and computer sciences*, vol. 35, pp. 607–616, 1995.
- [55] Curran, H.J.; Gaffuri, P.; Pitz, W.J.; Westbrook, C.K., "A comprehensive modeling study of iso-octane oxidation," *Combustion and Flame*, vol. 129, pp. 253–280, 2002.
- [56] Pope, S.B., "Computationally efficient implementation of combustion chemistry using in situ adaptive tabulation," *Combustion and Flame*, vol. 1, pp. 41–63, 1997.

- [57] Chen, J.-Y.; Blasco, J.A. ; Fueyo N. ; Dopazo, C., “An economical strategy for storage of chemical kinetics: Fitting in situ adaptive tabulation with artificial neural networks,” in *Twenty-Eighth Symposium (International) on Combustion*. The Combustion Institute, Pittsburgh, 2000, pp. 1–10.
- [58] Bongers, H.; van Oijen, J.A.; Somers, L.M.T.; de Goey, L.P.H., “The flamelet-generated manifold method applied to steady planar partially premixed counterflow flames,” *Combustion Science and Technology*, vol. ?, pp. ?, 2005.
- [59] Maas, U.; Pope, S.B., “Simplifying chemical kinetics: Intrinsic low-dimensional manifolds in composition space,” *Combustion and Flame*, vol. 88, pp. 239264, 1992.
- [60] Nafe, J.; Maas, U., “A general algorithm for improving ildms,” *COMBUSTION THEORY AND MODELLING*, vol. 6, pp. 697709, 2002.
- [61] Nafe, J.; Maas, U., “Hierarchical generation of ildms of higher hydrocarbons,” *Combustion and Flame*, vol. 135, pp. 17–26, 2003.
- [62] Friedman, J. H., “Multivariate adaptive regression splines,” *Annals of Statistics*, vol. 19, pp. 1–67, 1991.
- [63] Schwer, D.A.; Lu, P.; Green, W.H.Jr., “An adaptive chemistry approach to modeling complex kinetics in reacting flows,” *Combustion and Flame*, vol. 133, pp. 451–465, 2003.
- [64] Frenklach, M.; Harris, S.J., “Aerosol dynamics modeling using the method of moments,” *Journal of Colloid Interface Sciences*, vol. 118, pp. 252, 1987.
- [65] Mauss, F., *Entwicklung eines kinetischen Modells der Russbildung mit schneller Polymerisation*, Ph.D. thesis, RWTH Aachen, 1997.
- [66] Gut, A., *An Intermediate Course in Probability*, Springer Verlag, Berlin-Heidelberg, 1 edition, 1995.
- [67] Hautman, D.J.; Dryer, F.L.; Schug, K.P.; Glassman, I., “A multiple step overall kinetic mechanism for the oxidation of hydrocarbons,” *Combustion Science and Technology*, vol. 25, pp. 219–235, 1981.
- [68] Peters, N.; Williams, F.A., *The Systematic Structure of Methane Flames. Part I: Stoichiometric Flames.*, Springer-Verlag, Berlin, 1987, Springer Series in Chemical Physics: Complex Chemical Reaction SYStems.

- Mathematical Modelling and Simulation., ed.: Warnatz, J. and Jäger, W.
- [69] Peters, N., “Systematic reduction of flame kinetics: Principles and details,” *Progress in Astronautics and Aeronautics Series: Dynamics of Reactive Systems. Part I: Flames*, vol. 113, pp. 67–86, 1988, AIAA, Washington, DC,.
- [70] Zhou, X., “Wavelets-galerkin scheme for a stokes problem,” *Numerical Methods for Partial Differential Equations*, vol. 20, pp. 193–198, 2002.
- [71] Czarski, T.; Pozniak, K.T.; Romaniuk, R.S.; Simrock, S., “Tesla cavity modeling and digital implementation in fpga technology for control system development,” *Nuclear Instruments and Methods in Physics Research Section A: Accelerators, Spectrometers, Detectors and Associated Equipment*, vol. 556:2, pp. 565–576, 2006.
- [72] Svenson, J., *Thermal decomposition of biomass and construction materials - an experimental study -*, Ph.D. thesis, Department of Chemistry, Göteborg University, 2004.
- [73] Myren, C. ; Hönell, C. ; Björnbom, E. ; Sjöström, K., “Catalytic tar decomposition of biomass pyrolysis gas with a combination of dolomite and silica,” *Biomass and Bioenergy*, vol. 23, pp. 217–227, 2002.
- [74] Zanzi, R.; Sjöström, K.; Björnbom, E. , “Rapid pyrolysis of agricultural residues at high temperature,” *Biomass and Bioenergy*, vol. 25, pp. 357–366, 2002.
- [75] Encinar, J.M.; Beltran, F.J.; Bernalte, A.; Ramiro, A.; Gonzalez J.F., “Pyrolysis of two agricultural residues: Olive and grape bagasse. influence of particle size and temperature,” *Biomass and Bioenergy*, vol. 11, pp. 397–409, 1996.
- [76] Lavric, E.D. ; Konnov, A.A.; De Ruyck, J., “Dioxin levels in wood combustion - a review,” *Biomass and Bioenergy*, vol. 26, pp. 115–145, 2004.
- [77] Beyler, C.L.; Hirschler, M., *Thermal Decomposition of Polymers*, The SFPE Handbook of Fire Protection Engineering, 3 edition, 2002.
- [78] Wade, C.A., “Study report, no. 92 (revised 2003),branzfire technical reference guide,” Tech. Rep. 92, BRANZ, 2003.

- [79] W.W. Jones, "State of the art in zone modeling of fires," Tech. Rep., National Institute of Standards and Technology, 2001.
- [80] Lahaye; J.; Prado; G., *In: Particulate Carbon Formation During Combustion*, chapter Morphology and Internal Structure of Soot and Carbon Blacks, Plenum Press, 3 edition, 1981.
- [81] McKinnon, J.T.; Howard, J.B., "The roles of pah and acetylene in soot nucleation and growth," in *Twenty-Fourth Symposium (International) on Combustion*. The Combustion Institute, Pittsburgh, 1992, pp. 965–971.
- [82] Hindsgaul, C.; Schramm, J.; Gratz, L.; Henriksen, U.; Bentzen, J.D., "Physical and chemical characterization of particles in producer gas from wood chips," *Bioresource Technology*, vol. 73, pp. 147–155, 2000.
- [83] Megaridis, C.M.; Dobbins, R.A., "Soot aerosol dynamics in a laminar ethylene diffusion flame," in *Twenty-Second Symposium (International) on Combustion*. The Combustion Institute, Pittsburgh, 1988, pp. 353–362.
- [84] Harris, S.J. ; Kennedy, I.M., "The coagulation of soot particles with van der waals forces," *Combustion Science and Technology*, vol. 59, pp. 443–454, 1988.
- [85] Wagner, H. Gg., *Soot in Combustion Systems and its Toxic Properties*, Plenum Press, New York, 1983.
- [86] Frenklach, M.; Wang, H., "Detailed modeling of soot particle nucleation and growth," in *Twenty-Third Symposium (International) on Combustion*. The Combustion Institute, Pittsburgh, 1990, p. 1559.
- [87] Mulholland, G.W., "Global soot growth model," *Fire safety science*, pp. 709–718, 1986.
- [88] Mountain, R.D.; Mulholland, G.W., "Light scattering from simulated smoke agglomerates," *Langmuir*, vol. 4, pp. 1321–1326, 1988.
- [89] Mulholland, G.W.; Samson, J.R.; Mountain, R.D. ; Gentry, J.W., "Cluster size distribution for free molecular and continuum flow regimes," *Energy Fuels*, vol. 2, pp. 481–486, 1988.
- [90] Butler, K.M.; Mulholland, G.W., "Generation and transport of smoke components," *Fire Technology*, vol. 40, pp. 149–176, 2004.

- [91] Cai, J.; Lu, N.; Sorensen, C.M., "Analysis of fractal cluster morphology parameters: Structural coefficient and density autocorrelation function cutoff," *Journal of Colloid and Interface Science*, vol. 171, pp. 470–473, 1995.
- [92] Kazakov, A.; Frenklach, M., "Soot particle coagulation and aggregation," *Combustion and Flame*, vol. 114, pp. 484–501, 1998.
- [93] Kim, C.H. ; El-Leathy, A.M. ; Xu,F. ; Faeth, G.M, "Soot surface growth and oxidation in laminar diffusion flames at pressures of 0.1-1.0 atm," *Combustion and Flame*, vol. 136, pp. 191–207, 2004.
- [94] Kennedy, I .M., "Models of soot formation and oxidation," *Progress in Energy and Combustion Science*, vol. 23, pp. 95, 1997.
- [95] Calcote, H.F.; Manos, D.M., "Effect of molecular structure on incipient soot formation," *Combustion and Flame*, vol. 49, pp. 289, 1983.
- [96] Haynes, B.S.; Wagner, H. GG., "Soot formation," *Progress in Energy and Combustion Science*, vol. 7, pp. 229–273, 1981.
- [97] Gill, R.J.; Olson, D.B., "Estimation of soot thresholds for fuel mixtures," *Combustion Science and Technology*, vol. 40, pp. 307–315, 1984.
- [98] Takahashi, F.; Glassman, I., "Sooting correlations for premixed flames," *Combustion Science and Technology*, vol. 37, pp. 1–19, 1984.
- [99] Kahn, I.M.; Greeves, G.; Probert, D.M., "?," *Air Pollution Control in transport Engines*, vol. C142/71, pp. 205–217, 1971, The Institution of Mechanical Engineers, London.
- [100] Lefebvre, A., "Flame radiation in gas turbine combustion chambers," *Int. J. Heat and Mass Transfer*, vol. 27, pp. 1493–1510, 1984.
- [101] De Ris, J., "Prediction of fire dynamics," *US Department of Commerce, Building and Fire Research Laboratory, NIST-GCR-97-729*, vol. 0, pp. 0–40, 1997.
- [102] Markstein; De Ris, J., "Wall-fire radiant emission- part 2: Radiation and heat transfer from porous-metal wall burner flames," in *Twenty-Fourth Symposium (International) on Combustion*. The Combustion Institute, Pittsburgh, 1992, pp. 1747–1752.
- [103] Tesner, P.A.; Snegiriova, T.D.; Korre, V.G., "Kinetics of dispersed carbon formation," *Combustion and Flame*, vol. 17, pp. 253–260, 1997.

- [104] Tesner, P.A.; Tsygankova, E.I.; Guilazetdinov, L.P.; Zuyev, V.P.; Loshakova, G.V., "The formation of soot from aromatic hydrocabons in diffusion flames of hydrocarbon-hydrogen mixtures," *Combustion and Flame*, vol. 17, pp. 279–285, 1971.
- [105] Surovikin, V.F., "Analytical description of the process of nucleus-formation and growth of particles of carbon black in the thermal decomposition of aromatic hydrocarbons in the gas phase," *Khimiya Tverdogo Topлива*, vol. 10, pp. 111–122, 1976.
- [106] Magnussen, B.F.; Hjertager, B.H.; Olsen, J.G.; Bhaduri, D., "Effects of turbulent structure and local concentrations on soot formation and combustion in C_2H_2 diffusion flames," in *Sixteenth Symposium (International) on Combustion*. The Combustion Institute, Pittsburgh, 1976, p. 719.
- [107] Brown, A.J.; Heywood, J.B., "A fundamentally-based stochastic mixing model methos for predicting *no* and soot emissions from direct injection diesel engines," *Combustion Science and Technology*, vol. 58, pp. 195–207, 1988.
- [108] Jensen, D.E., "Prediction of soot formation rates: a new approach," 1974.
- [109] Graham, S.C., "The modelling of the growth of soot particles during the pyrolysis and partial oxidation of aromatic hydrocarbons," 1981.
- [110] Moss, J.B.; Steward, C.D.; Syed, K.J., "Flow field modelling of soot formation at elevated pressures," in *Twenty-Second Symposium (International) on Combustion*. The Combustion Institute, Pittsburgh, 1988, pp. 413–423.
- [111] Young, K.J.; Steward, C.D.; Moss, J.B., , in *Twenty-Fifth Symposium (International) on Combustion*, 1994.
- [112] Syed, K. J.; Steward, C.D.; Moss, J.B., "Modelling soot formation and thermal radiation in buoyant turbulent diffusion flames," in *Twenty-Third Symposium (International) on Combustion*. The Combustion Institute, Pittsburgh, 1992, pp. 1533–1541.
- [113] Fairweather, M.; Jones, W.P.; Lindstedt, P., "Predictions of radiative transfer from turbulent reacting jet in a cross-wind," *Combustion and Flame*, vol. 89, pp. 45–63, 1992.

- [114] Lindstedt, P.D., *A simple reaction mechanism for soot formation in non-premixed flames*, Springer Verlag Berlin, 1992, Aerosynamics in Combustion.
- [115] Fairweather, M.; Jones, W.P.; Ledin, H.S.; Lindstedt, P., "Predictions of soot formation in turbulent non-premixed propane flames," in *Twenty-Fourth Symposium (International) on Combustion*. The Combustion Institute, 1992, pp. 1067–1074.
- [116] Nagel, J.; Strickland-Constable, R.F., *Fifth Carbon Conference*, vol. 1, Pergamon Oxford, 1962.
- [117] Smooke, M.D.; Puri, I.K.; Seshadri, K., "A comparison between numerical calculations and experimental measurements of the structure of a counterflow diffusion flame burning diluted methane in diluted air," in *Twenty-First Symposium (International) on Combustion*. The Combustion Institute, Pittsburgh, 1986, pp. 1783–1792.
- [118] Kollmann, W.; Kennedy, I. M.; Metternich, M.; Chen, J.-Y., *Soot Formation in Combustion - Mechanisms and Models*, Springer Verlag, Berlin-Heidelberg, 1 edition, 1994.
- [119] Moss, J.B.; Steward, C.D., "Flamelet-based smoke properties for the field modelling of fires," *Fire Safety Journal*, vol. 30, pp. 229–250, 1998.
- [120] Harris, S.J.; Weiner, A.M., "Surface growth of soot particles in premixed ethylene/air flames," *Combustion Science and Technology*, vol. 31, pp. 155–167, 1983.
- [121] Neimark, A.V.; Köylü, Ü.Ö.; Rosner, D.E., "Extended characterization of combustion-generated aggregates: Self-affinity and lacunarity," *Journal of Colloid and Interface Science*, vol. 180, pp. 590–597, 1996.
- [122] C.J. Dasch, "The decay of soot surface growth reactivity and its importance in total soot formation," *Combustion and Flame*, vol. 61, pp. 219–225, 1985.
- [123] Wersborg, B.L.; Howard, J.B.; Williams, G.C., "Physical mechanism in carbon formation flames," in *Fourteenth Symposium (International) on Combustion*. The Combustion Institute, Pittsburgh, 1973, pp. 929–940.
- [124] Colket, M.B.; Hall, R.J., in *Soot Formation in Combustion*, chapter Success and uncertainties in Modeling Soot Formation in Laminar, Premixed Flames, pp. 442–470, Springer Verlag, Berlin-Heidelberg, 1 edition, 1994.

- [125] Harris, S.J.; Weiner, A.M., "Chemical kinetics of soot particle surface growth," *Annual Review of Physical Chemistry*, vol. 36, pp. 31–52, 1985.
- [126] Harris, S.J.; Weiner, A.M., "?," *Combustion Science and Technology*, vol. 31, pp. 267, 1983.
- [127] Smoluchowski, M.V., "?," *Z. phys. Chem.*, vol. 92, pp. 129, 1917.
- [128] Appel, J.; Bockhorn, H.; Frenklach, M., "Kinetic model of soot formation with detailed chemistry and physics: Laminar premixed flames of c_2 hydrocarbons," *Combustion and Flame*, vol. 121, pp. 122–136, 2000.
- [129] Frenklach, M.; Wang, H., *Soot Formation in Combustion*, chapter Detailed Mechanism and Modeling of Soot Particle Formation, pp. 165–192, Springer Verlag, Berlin-Heidelberg, 1 edition, 1994.
- [130] Xu, F.; Faeth, G.M., "Soot formation in laminar acetylene/air diffusion flames at atmospheric pressure," *Combustion and Flame*, vol. 125, pp. 804–819, 2001.
- [131] Young, K.J.; Steward, C.D.; Moss, J.B., "Soot formation on confined turbulent flames fuelled by pre-vaporized kerosene and by ethylene," in *Proceedings of the Tenth International Symposium on Air Breathing Engines*, 1991, pp. 239–248.
- [132] Harris, S.J.; Kennedy, I.M., "Soot particle aerosol dynamics at high pressure," *Combustion and Flame*, vol. 78, pp. 390–397, 1989.
- [133] Fuchs, N.A., Ed., *Mechanics of Aerosols*, Pergamon New York, 1 edition, 1964.
- [134] Pratsini, S.E., "Simultaneous nucleation, condensation and coagulation in aerosols reactors," *Journal of Colloid and Interface Science*, vol. 124, pp. 416–427, 1987.
- [135] Köylü, Ü.Ö.; Xing, Y.; Rosner, D.E., "Fractal morphology analysis of combustion generated aggregates using angular light scattering and electron microscope images," *Langmuir*, vol. 11, pp. 4848–4854, 1995.
- [136] Mountain, R.D.; Mulholland, G.W.; Baum, H., "Simulation of aerosol agglomeration in the free-molecular and continuum flow regimes," *J. Colloid Interface Sci.*, vol. 114, pp. 67, 1986.
- [137] Mandelbrot, B.B., *The Fractal Geometry of Nature*, Freeman, New York, 1 edition, 1983.

- [138] Dobbins, R.A.; Santorro, R.J.; Semeerjian, H.G., "Analysis of light scattering from soot using optical cross sections for aggregates," in *Twenty-Third Symposium (International) on Combustion*, Combustion Institute, 1991, pp. 1525–1532.
- [139] Rogak, S.N.; Flagan, R.C.; Nguyen, H.V., "The mobility and structure of aerosol agglomerates," *Aerosol Science and Technology*, vol. 18, pp. 25–47, 1993.
- [140] Kruis, F.E.; Kusters, K.A.; Pratsinis, S.E., "A simple model for the evolution of the characteristics of aggregate particles undergoing coagulation and sintering," *Aerosol Science and Technol*, vol. 19, pp. 514–526, 1993.
- [141] Mitchell, P.; Frenklach, M., "Particle aggregation with simultaneous surface growth," *Physical Review E*, vol. 67, pp. 1–11, 2003.
- [142] Dobbins, R.A., "Soot inception temperature and the carbonization rate of precursor particles," *Combustion and Flame*, vol. 130, pp. 204–214, 2002.
- [143] Balthasar, M.; Frenklach, M., "Detailed kinetic modeling of soot aggregate formation in laminar premixed flames," *Combustion and Flame*, vol. 140, pp. 130–145, 2005.
- [144] Gelbard, F.; Seinfeld, J.H., "The general dynamic equation of aerosols," *Journal of Colloid and Interface Science*, vol. 68, pp. 363–382, 1978.
- [145] Colket, M.B.; Hall, R.J.; Sangiovanni, J.J.; Seery, D.J., "The determining of rate-limiting steps during soot formation," Tech. Rep., United Technology Research Center, East Hartford, CT 06108, 1991, UTC Report No. UTCRC91-21.
- [146] Goel, A.; Howard, J. B., "Reaction rate coefficient of fullerene (c_{60}) consumption by soot," *Carbon*, vol. 41, pp. 1949–1954, 2003.
- [147] Radke, L.F.; Hegg, A.S.; Hobbs, P.V.; Penner, J.E., "Effects of aging on the smoke from a large forest fire," *Atmospheric Research*, vol. 38, pp. 315–332, 1995.
- [148] Efendiev, Y.; Struchtrup, H.; Luskin, M.; Zachariah, M.R., "A hybrid sectional-moment model for coagulation and phase segregation in binary liquid nanodroplets," *Journal of Nanoparticle Research*, vol. 11, no. 1-2, pp. 61–72, 2002.

- [149] Smith, D.M.; Chughtai, A.R., "The surface structure and reactivity of black carbon," *Colloids and Surfaces A*, vol. 105, pp. 47–77, 1995.
- [150] Galloway, F. M.; Hirschler, M. M., "A model for the spontaneous removal of airborne hydrogen chloride by common surfaces," *Combustion and Flame*, vol. 14, pp. 203–307, 1989, no 4.
- [151] Jones, W.W., "A model for the transport of fire, smoke and toxic gases," Tech. Rep., National Bureau of Standards, 1984, NBSIR 84-2934.
- [152] Chughtai, A.R.; Atteya, M.O.; Konowalchuk, B.K.; Smith, D.M., "Adsorption and adsorbate interaction at soot particle surfaces," *Carbon*, vol. 36, pp. 1573–1589, 1998.
- [153] Decesari, S.; Faccini, M.C.; Matta, E.; Mircea, M.; Fuzzi, S.; Chughtai, A.R.; Smith, D.M., "Water soluble organic compounds formed by oxidation of soot," *Atmospheric Environment*, vol. 36, pp. 1827–1832, 2002.
- [154] Jones, C.C.; Chughtai, A.R.; Murugaverl, B.; Smith, D.M., "Effects of air/fuel combustion ratio on the polycyclic aromatic hydrocarbon content of carbonaceous soots from selected fuels," *Carbon*, vol. 42, pp. 2471–2484, 2004.
- [155] Howard, J.B.; William, J.K.Jr., "Soot control by fuel additives," *Progress in Energy and Combustion Science*, vol. 6, pp. 263–276, 1980.
- [156] L. Bagnetto, "Smoke abatement in gas turbines. part 2: Effect of fuels, additives, and operating conditions on smoke emissions and flame radiation," Summary report, contract no. n00156-67-c-2351, U.S. Naval Air Systems Command, 1968.
- [157] D.W. Golothan, "Diesel engine exhaust smoke: the influence properties and the effects of using a barium containing fuel additive," *SAE paper*, , no. 670092, pp. 1, 1967.
- [158] Cotton, D.H.; Friswell, N.J.; Jenkins, D.R., "The suppression of soot emission from flames by metal additives," *Combustion and Flame*, vol. 17, pp. 87–98, 1971.
- [159] B. Toone, *Combustion in advanced gas turbine systems*, vol. 10 of *Cranfield International Symposium Series*, chapter A review of aero engine smoke emission, Pergamon Press, 1968.

- [160] Fiorello, S.C., "The navy's smoke abatement program," in *SAE paper No. 680345*, 1968.
- [161] R.M. Shirmer, *Emissions from continuous combustion systems*, chapter Effect of fuel composition on particulate emissions from gas turbine engines, Plenum Press, N.Y., 1972.
- [162] Ray, S.K.; Long, R., "Polycyclic aromatic hydrocarbons from diffusion flames and diesel engine combustion," *Combustion and Flame*, vol. 8, pp. 139–151, 1964.
- [163] Weeks, R.L.; Clinkenbeard, W.L.; Solties, J.D., "," in *Proceedings of the fifth World Petroleum Congress*. World Petroleum Council, 1959, p. 381.
- [164] J. Vaerman, "," *Journal of the Institute of Petroleum*, vol. 50, pp. 155, 1964.
- [165] Kukin, I., "," *Environmental Sciences and Tehnologies*, vol. 7(7), pp. 606, 1973.
- [166] W.C. Hinds, *Aerosol technology: properties, behaviour, and measurement of airborne particles*, John Wiley & Sons, 1982.
- [167] Chughtai, A.R.; Williams, G.R.; Atteya, N.J.; Miller, N.J.; Smith, D.M., "Carbonaceous particle hydration," *Atmospheric Environment*, vol. 33, pp. 2679–2687, 1999.
- [168] Chughtai, A.R.; Miller, N.J.; Smith, D.M.; Pitts, J.R., "Carbonaceous particle hydration iii," *Journal of Atmospheric Chemistry*, vol. 34, pp. 259–279, 1999.
- [169] Willis, K. D.; Orme, M. E. , "Experiments on the dynamics of droplet collisions in a vacuum," *Experiments in Fluids*, vol. 29, no. 4, pp. 347–358, 2000.
- [170] Norris, J.R., "Smoluchowski's coagulation equation: uniqueness, nonuniqueness and a hydrodynamic limit for the stochastic coalescent," *The Annals of Applied Probability*, vol. 9, pp. 78–109, 1999.
- [171] R. McGraw, "Description of aerosol dynamics by the quadrature method of moments," *Aerosol Science and Technology*, vol. 27, pp. 255–265, 1997.
- [172] Maetzing, H.; Baumann, W.; Paur, H.-R., "Bimodal aerosol coagulation with simultaneous condensation/evaporation," *Journal of Aerosol Science*, vol. 27, no. Supplement1, pp. S363–S364, 1996.

- [173] Pope, C.J.; Howard, J.B., "Simultaneous particle and molecule modeling (spamm): An approach for combining sectional aerosol equations and elementary gas-phase reactions," *Aerosol Science and Technology*, vol. 27, pp. 73–94, 1997.
- [174] Carlsson, J.; Husted, B.; Goransson, U.; Dederichs, A.S. , "Anwendung von cfd-programmen fr brandtechnische berechnungen.," *Zeitschrift fr Forschung und Technik im Brandschutz VFDB*, vol. 5, pp. 70–77, 2006.
- [175] H.J. Gerhardt, "Entrauchungsnachweise - kritische diskussion von methoden des brandschutzingenieurwesens," *Zeitschrift fr Forschung und Technik im Brandschutz VFDB*, , no. 3, pp. 99–104, 2001.
- [176] Blomqvist , P., *Emission from fires- consequences for human safety and the environment*, Ph.D. thesis, Lund University, 2005, Report LUTVDG/TVBB-1030-SE.
- [177] Xu,F. ; Kim, C.H. ; El-Leathy, A.M. ; Faeth, G.M, "Soot surface oxidation in hydrocarbon/air diffusion flames at atmospheric pressure," *Combustion and Flame*, vol. 132, pp. 43–57, 2003.
- [178] Hofmann, A.; Holmstedt, G., "Analys av brandrester vid anlagd brand," *Brandforsk*, vol. 203-031, pp. 1, 2006.